

**UNCLASSIFIED**

---

---

**AD 262 211**

---

*Reproduced  
by the*

**ARMED SERVICES TECHNICAL INFORMATION AGENCY  
ARLINGTON HALL STATION  
ARLINGTON 12, VIRGINIA**



---

---

**UNCLASSIFIED**

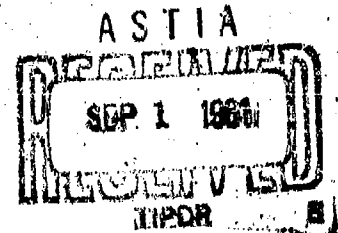
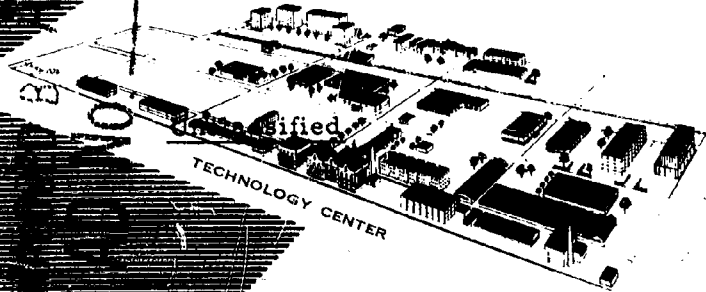
**NOTICE:** When government or other drawings, specifications or other data are used for any purpose other than in connection with a definitely related government procurement operation, the U. S. Government thereby incurs no responsibility, nor any obligation whatsoever; and the fact that the Government may have formulated, furnished, or in any way supplied the said drawings, specifications, or other data is not to be regarded by implication or otherwise as in any manner licensing the holder or any other person or corporation, or conveying any rights or permission to manufacture, use or sell any patented invention that may in any way be related thereto.

11262211

ARF

ARF 1158A01-5  
(Final Report)

ARMOUR RESEARCH FOUNDATION OF ILLINOIS INSTITUTE OF TECHNOLOGY



Contract NBy-3185

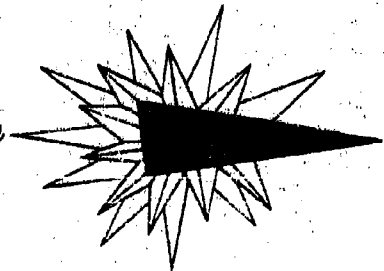
Sponsored by:

The Navy Department  
Bureau of Yards and Docks  
U. S. Naval Civil Engineering Laboratory  
Port Hueneme, California

RADIATION STREAMING IN SHELTER ENTRANCEWAYS

July, 1961

*25 years of research*



44-4.3  
XEROX

ARF 1158A01-5

Final Report

RADIATION STREAMING IN SHELTER ENTRANCEWAYS

Sponsored by:

The Navy Department  
Bureau of Yards and Docks  
U. S. Naval Civil Engineering Laboratory  
Port Hueneme, California  
Attention: Capt. A. B. Chilton, CEC, USN  
Navy Contract NBy-3185

Report Written by:

C. W. Terrell  
and  
A. J. Jerri

Project Personnel:

C. W. Terrell (Project Leader)  
A. J. Jerri  
R. O. Lyday, Jr.

ARMOUR RESEARCH FOUNDATION  
of  
Illinois Institute of Technology

July, 1961

ARMOUR RESEARCH FOUNDATION OF ILLINOIS INSTITUTE OF TECHNOLOGY

The authors wish to acknowledge the interest and assistance of other ARF groups, particularly members of the Reactor Operations and Health Physics Section and the Metallurgy and Shop staff for the preparation of the radiation sources.

Work performed on this project is contained in logbooks: C10797, C10803, C10807, C10817, C10862, C10989, C11056, and C11161.

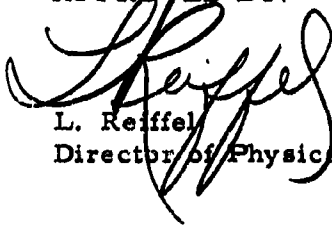
Respectfully submitted,

ARMOUR RESEARCH FOUNDATION  
of Illinois Institute of Technology



C. W. Terrell, Research Supervisor

APPROVED BY:



L. Reiffel  
Director of Physical Research

Contract NBy-3185  
ARF 1158A01-5  
Final Report

REPORT DISTRIBUTION LIST

<u>No. of Copies</u>	<u>Recipient</u>
1	Chief, Bureau of Yards and Docks Department of the Navy Washington 25, D. C.
1	Dr. Lewis V. Spencer National Bureau of Standards Washington 25, D. C.
1	Mr. John Auxler Oak Ridge National Laboratory Oak Ridge, Tennessee
1	Dr. James O. Buchanan Office of Civil and Defense Mobilization Battle Creek, Michigan
1	Mr. Charles M. Eisenhauer Radiation Physics Laboratory High Voltage Laboratory National Bureau of Standards Washington 25, D. C.
1	Mrs. Shea L. Kruegel, CRTZS Cambridge Research Center Bedford, Massachusetts
1	Major F. A. Verser, U. S. A. Defense Atomic Support Agency Washington 25, D. C.
1	Dr. Ronald Shephard University of California Engineering Field Station 1301 South 46th Street Richmond 4, California

REPORT DISTRIBUTION LIST (continued)

<u>No. of Copies</u>	<u>Recipient</u>
3	Mr. L. Neal FitzSimons Office of Civil and Defense Mobilization Winder Building Washington 25, D. C.
3	Dr. William Kreger U. S. Naval Radiological Defense Laboratory San Francisco 24, California
1	Mr. Richard Park National Academy of Sciences 2101 Constitution Avenue Washington 25, D. C.
1	Mr. E. E. Shalowitz Protective Construction GSA Building 19th and F Street, N. W. Washington 25, D. C.
10	Capt. A. B. Chilton, CEC, USN U. S. Naval Civil Engineering Laboratory Port Hueneme, California
1	Mr. G. H. Albright The Pennsylvania State University College of Engineering and Architecture University Park, Pennsylvania
1	CDR W. J. Christensen, CEC, USN Bureau of Yards and Docks, Code D-440 Washington 25, D. C.
1	LCDR E. M. Saunders, CEC, USN NROTC Unit Stanford University Palo Alto, California
2	LCDR J. C. LeDoux, CEC, USN U. S. Naval School, CEC Officers Port Hueneme, California

REPORT DISTRIBUTION LIST (continued)

<u>No. of Copies</u>	<u>Recipient</u>
2	Commanding Officer U. S. Chemical Corps Research and Development Command Washington 25, D. C.
1	Chief, Defense Atomic Support Agency Washington 25, D. C.
1	Officer in Charge CECOS (ATTN: ADCE Course) Port Hueneme, California
3	Director, Civil Effects Test Group Atomic Energy Commission (ATTN: Mr. R. L. Corbie) Washington 25, D. C.
3	U. S. Atomic Energy Commission Technical Information Service P. O. Box 62 Oak Ridge, Tennessee
3	Commanding Officer Nuclear Defense Laboratory Army Chemical Center Edgewood, Maryland
1	Commanding Officer and Director Naval Research and Development Laboratory San Francisco, California
1	Technical Operations, Inc. (Contractor) Attn: Dr. Clarke Burlington, Massachusetts
25	Naval Civil Engineering Laboratory Port Hueneme, California

REPORT DISTRIBUTION LIST (continued)

<u>No. of Copies</u>	<u>Recipient</u>
1	ARF Report Library via K. W. Miller
1	ARF Main Files
1	ARF Physics (A) Division Files via L. Reiffel and P. H. Wyckoff
20	ARF Reactor Physics Section Files via C. W. Terrell

## ABSTRACT

This document is the Final Report on ARF Project 1158A01, sponsored by the Bureau of Yards and Docks. The report covers the second year of the program.

The objective of the program is an analytical and experimental investigation of nuclear radiation streaming in ducts and shelter entranceways.

In the program just completed the energy dependence of duct attenuation was extended for gamma rays. Further duct geometry dependence was also measured. Thermal neutron attenuation was determined for a non-point source and the neutron attenuation was found to be extremely small.

Use of albedo theory to successfully describe the radiation streaming of gamma rays was further strengthened and a computer code was prepared to describe the streaming in a straight duct. The code will represent a tremendous labor saving device for future calculations. An analytical analysis of a straight duct, using albedo theory, is included in the appendix along with an outline of future research needs.

## TABLE OF CONTENTS

	<u>Page No.</u>
ABSTRACT	viii
List of Illustrations	xi
List of Tables	xiv
I. INTRODUCTION . . . . .	1
II. SUMMARY OF PRIOR WORK . . . . .	3
A. Differential Neutron Albedo Data	3
III. ANALYTICAL PROGRAM . . . . .	6
A. Introduction	6
B. Albedo Theory	7
1. Cosine Re-emission Distribution	7
2. Isotropic Re-emission Distribution	9
C. Albedo Data	11
1. Gamma Rays	11
2. Neutrons	12
D. Programming Notes	12
E. Code Input Data	13
F. Sample Problem	15
IV. EXPERIMENTAL PROGRAM . . . . .	17
A. Description of Experiments	17
B. Gamma Dose Rate Distribution Measurements	17
1. Sources	21
2. Detectors	22
3. Results	24
a. Sodium Source Measurements	24
b. Gold Source Measurements	36
4. Analysis and Comparison	36
C. Relative Worth of the Four Scattering Surfaces which Form the Right Angle Bend	49

TABLE OF CONTENTS (continued)

	<u>Page No.</u>
D. Thermal Neutron Flux Distribution Measurements from a Plane Thermal Source	56
1. Source	57
2. Detectors	59
3. Source Distribution	60
4. Thermal Neutron Distribution Measurements - Results	60
V SUMMARY AND CONCLUSIONS . . . . .	68

APPENDICES

I. BIBLIOGRAPHY	70
II. FUTURE RESEARCH RECOMMENDATIONS	75
III. SEMI-RIGOROUS ALBEDO ANALYSIS IN A STRAIGHT DUCT	78
IV. IT AND FORTRAN COMPUTER PROGRAMS	94

## LIST OF ILLUSTRATIONS

<u>Figure No.</u>		<u>Page No.</u>
1.	Fraction of Incident Neutrons Which are Reflected from a Semi-Infinite, Isotropic Scattering Absorbing Medium	5
2.	Geometry Used by Computer Program to Calculate Doses and Fluxes in Straight Rectangular Ducts	8
3.	Assembled Concrete Entranceway	18
4.	Concrete Entranceway with Roof Section Removed	19
5.	Concrete Entranceway Partially Assembled	20
6.	Photograph of Detection Equipment	23
7.	Gamma Dose Rate Distribution Measurements	25
8.	Measured Gamma Dose Rate Distribution in 6 by 6 Foot Concrete Entranceway with Single Right Angle Bend	28
9.	Measured Gamma Dose Rate Distribution in 6 by 6 Foot Concrete Entranceway with Single Right Angle Bend	29
10.	Measured Gamma Dose Rate Distribution in 6 by 6 Foot Concrete Entranceway with Single Right Angle Bend	31
11.	Measured Gamma Dose Rate Distribution in 6 by 6 Foot Concrete Entranceway with Single Right Angle Bend	32
12.	Measured Gamma Dose Rate Distribution in 6 by 6 Foot Concrete Entranceway with Single Right Angle Bend	34
13.	Measured Gamma Dose Rate Centerline Distribution in 6 by 6 Foot Concrete Entranceway with Single Right Angle Bend	35

LIST OF ILLUSTRATIONS (continued)

<u>Figure No.</u>		<u>Page No.</u>
14.	Measured Gamma Dose Rate Centerline Distribution in 6 by 6 Foot Concrete Entranceway with Single Right Angle Bend	38
15.	Measured Gamma Dose Rate Centerline Distribution in 6 by 6 Foot Concrete Entranceway with Single Right Angle Bend	39
16.	Measured Gamma Dose Rate Centerline Distribution in 6 by 6 Foot Concrete Entranceway with Single Right Angle Bend	41
17.	Measured Gamma Dose Rate Centerline Distribution in 6 by 6 Foot Concrete Entranceway with Single Right Angle Bend	42
18.	Measured Gamma Dose Rate Centerline Distribution in 6 by 6 Foot Concrete Entranceway with Single Right Angle Bend	44
19.	Measured Gamma Dose Rate Centerline Distribution in 6 by 6 Foot Concrete Entranceway with Single Right Angle Bend	45
20.	Comparison of First Leg ( $L_1$ ) Centerline Gamma Dose Rate Distributions for Au, Co, and Na	47
21.	Comparison of Second Leg ( $L_2$ ) Centerline Gamma Dose Rate Distributions for Au, Co, and Na	48
22.	Experimental Geometry for Determining Contributions from Scattering Surfaces which Form Right Angle Bend of 6 by 6 Foot Concrete Entranceway	52
23.	Thermal Neutron Distribution Measurements	58
24.	Thermal Neutron Distribution from Graphite Thermal Column Face	62
25.	Measured Thermal Neutron Flux Centerline Distribution in 6 by 6 Foot Concrete Entranceway with Single Right Angle Bend.	64

LIST OF ILLUSTRATIONS (continued)

<u>Figure No.</u>		<u>Page No.</u>
26.	Comparison of Thermal Neutron Flux Centerline Distributions for Point and Cosine Isotropic Thermal Neutron Sources	65

LIST OF TABLES

<u>Table No.</u>		<u>Page No.</u>
I.	Gamma Dose Rate Measurements in 6 by 6 Foot Concrete Entranceway - Na-24 Source at $S_{14}$	27
II.	Gamma Dose Rate Measurements in 6 by 6 Foot Concrete Entranceway - Na-24 Source at $S_{10}$	30
III.	Gamma Dose Rate Measurements in 6 by 6 Foot Concrete Entranceway - Na-24 Source at $S_7$	33
IV.	Gamma Dose Rate Measurements in 6 by 6 Foot Concrete Entranceway - Au-198 Source at $S_{14}$	37
V.	Gamma Dose Rate Measurements in 6 by 6 Foot Concrete Entranceway - Au-198 Source at $S_{10}$	40
VI.	Gamma Dose Rate Measurements in 6 by 6 Foot Concrete Entranceway - Au-198 Source at $S_7$	43
VII.	Dose Attenuation Ratios Versus Energy and Length of First Leg $l_1$	46
VIII.	Gamma Dose Attenuation Factors for Concrete Shelter Entranceway	50
IX.	Effect of Lead Sheet on Scattering Surface $A_3$	53
X.	Effect of Lead Sheet on Scattering Surface $A_1$	54
XI.	Thermal Neutron Source Distribution - Reactor Power 0.1 Watt	61
XII.	Measured Thermal Neutron Flux Centerline Distribution in 6 by 6 Foot Concrete Entranceway from Isotropic Cosine Thermal Neutron Source.	63

## RADIATION STREAMING IN SHELTER ENTRANCEWAYS

### I. INTRODUCTION

In recent years increasing emphasis has been placed on survival oriented research projects. Both the Military and the Civil Defense are concerned with the protection of personnel and property against nuclear attack in terms of hardened bases and personnel shelters. This project deals with the nuclear radiation aspect of the weapon's output and how this radiation behaves when allowed to fall on a shelter entranceway or duct.

When nuclear radiation is incident on a semi-infinite plane surface, containing the entrance to a duct or shelter entranceway, a certain quantity of the radiation will be transmitted. The quantity of the radiation transmitted will depend on the duct cross sectional area, number of bends, the bend angle, the length of each leg, the wall material, the energy and type of radiation and the nature of source, i. e., plane parallel, plane isotropic or point.

Investigation of the above parameters is the objective of this program. This document is a final report on the work done under Contract NBy-3185, sponsored by the Bureau of Yards and Docks, and summarizes the results of the second year scope of the contract covering the period October, 1960 to June, 1961.

Since the inception of the program in October, 1959, major emphasis has been placed on obtaining experimental data under sufficiently realistic

ARMOUR RESEARCH FOUNDATION OF ILLINOIS INSTITUTE OF TECHNOLOGY

conditions so that direct shelter and duct design criteria might be formulated. Existence of such measurements then allows analytical investigation to determine a general recipe to obtain the attenuation offer by any given design of duct or entranceway. The need for such research has been repeatedly stressed by others and need not be amplified here.

The Foundation is pleased to have the opportunity to conduct this investigation for the Navy and the individual staff members on the project look forward to continuing programs to complete the study in full.

## II. SUMMARY OF PRIOR WORK

In the previous report, ARF 1158-12, we summarized most of the analytical and experimental work done by others. We have recently uncovered an old report containing differential neutron albedo information. This work, done by Dr. S. W. Kash, who is now a member of our staff, is summarized briefly.

### A. Differential Neutron Albedo Data

Interesting information about neutron reflection from different materials, which can easily be related to the neutron number albedo, was reported by S. W. Kash<sup>1</sup>. Kash used Chandrasekhar's distribution expression for the reflection of a constant net flux falling perpendicularly on a semi-infinite, isotropic scattering, absorbing medium. On integrating overall perpendicular outward directions, the expressions for the total fraction of neutrons reflected from the semi-infinite medium, for an arbitrary incident angle of a parallel beam is

$$f(\mu_0, C) = 1 - (1 - C)^{1/2} H(\mu_0, C)$$

where

$\cos^{-1} \mu_0$  = angle of incidence

$C$  = ratio of scattering cross section to total cross section of the semi-infinite medium

$H(\mu_0, C)$  = Chandrasekhar's reflection distribution function.

---

<sup>1</sup> Kash, S. W., "Reflection of Neutrons by a Semi-Infinite, Isotropic Scattering, Absorbing Medium." NAA-SR-275, Reactor Physics Quarterly Progress Report, May-July, 1953.

This, as well as the single scattering fraction expression  $f_1(\mu_0, C)$ , are plotted in Figure 1. It should be noted that these expressions lack the angular scattering dependence in their derivation. Also, it is interesting to note that the single scattering approach is a closer approximation for highly absorbing materials.

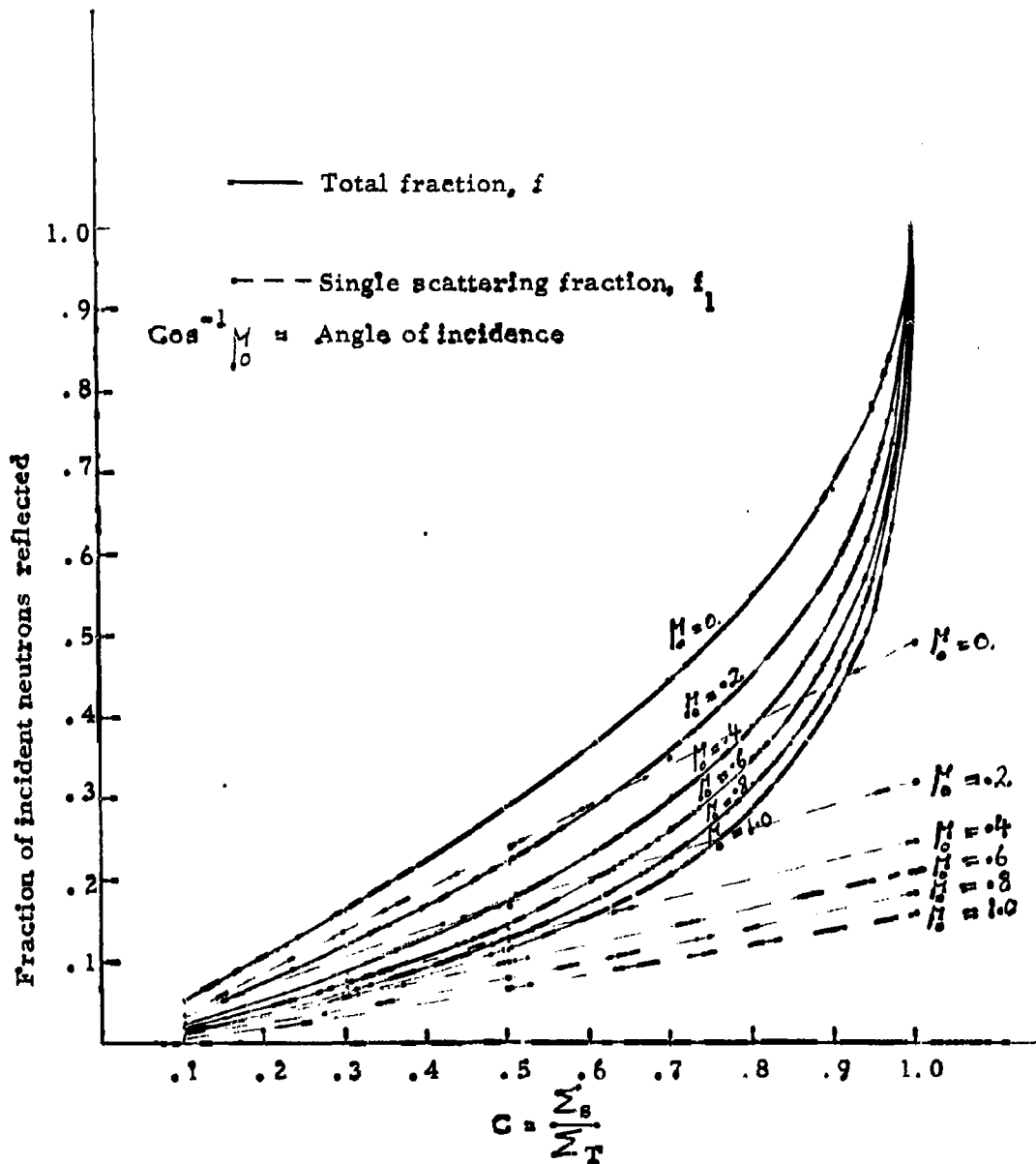


Figure 1. Fraction of Incident Neutrons which are Reflected from a Semi-infinite, Isotropic Scattering Absorbing Medium

### III. ANALYTICAL PROGRAM

#### A. Introduction

The problem of nuclear radiation transport through ducts and shelter entranceways may be approached in many different ways. The most practical approach is that which invokes the albedo recipe. The dose albedo is defined as the ratio of the dose emerging from a surface to the dose impinging upon the surface. For this approach to be satisfactory, angle and energy dependence of the albedo is needed. Monte Carlo calculated incident angle and energy dependent albedo values are available for gamma rays only, and with very little information about the re-emission distribution<sup>2</sup>. No such information is available for neutron albedos.

The albedo approach is the main analytical method adopted in most of the calculations done at ARF and has been programmed for the ARF Univac 1105. The program has also been prepared in Fortran and will calculate the gamma ray dose and neutron flux distribution along the centerline in a straight rectangular duct of any half width to length ratio, and for any source and detector centerline position.

One of a number of reasons for coding this calculation lies in the fact that the computation of a rectangular duct involves a double integration (see Appendix III), and requires many man hours of calculation of effort, especially when  $\delta/L$  is not small and no simple approximation for evaluating the integrals is realistic.

---

<sup>2</sup>. Berger, M. and D. Raso, "Backscattering of Gamma Rays," N. B. S. Report No. 5982 (July 24, 1958).  
ARMOUR RESEARCH FOUNDATION OF ILLINOIS INSTITUTE OF TECHNOLOGY

## B. Albedo Approach

The computer code utilizes the following analytical approach. In a rectangular duct of length  $l$  and half width  $\delta$ , as shown in Figure 2, let the source and detector centerline positions be at a distance  $L_1$  and  $L_2$  respectively from the entrance of a duct. For a point source strength  $kS_0$ , the direct contribution to the detector is:

$$\frac{kS_0}{4\pi(L_2 - L_1)^2}$$

The reflection contribution is to be treated for cosine or isotropic re-emission distribution or a combination of both.

### 1. Cosine Re-emission Distribution

The reflection contribution to the detector from a differential roof area  $dA$  located at  $(y, \delta, \theta)$

$$\frac{kS_0}{4\pi} \times \frac{1}{R_1^2} \times \frac{\delta}{R_1} \times \alpha'(\theta, \phi) \times A \times \frac{2\delta}{R_2} \times \frac{1}{2\pi R_2} \times dA'$$

where

$$R_1^2 = (y - L_1)^2 + \delta^2 \sec^2 \theta$$

$$R_2^2 = (y - L_2)^2 + \delta^2 \sec^2 \theta$$

$A$  is the fraction of the total re-emission distribution which is cosine.

$\alpha'$  is the albedo based on the first reflection

$$dA' = dx dy = \delta \sec^2 \theta d\theta dy.$$

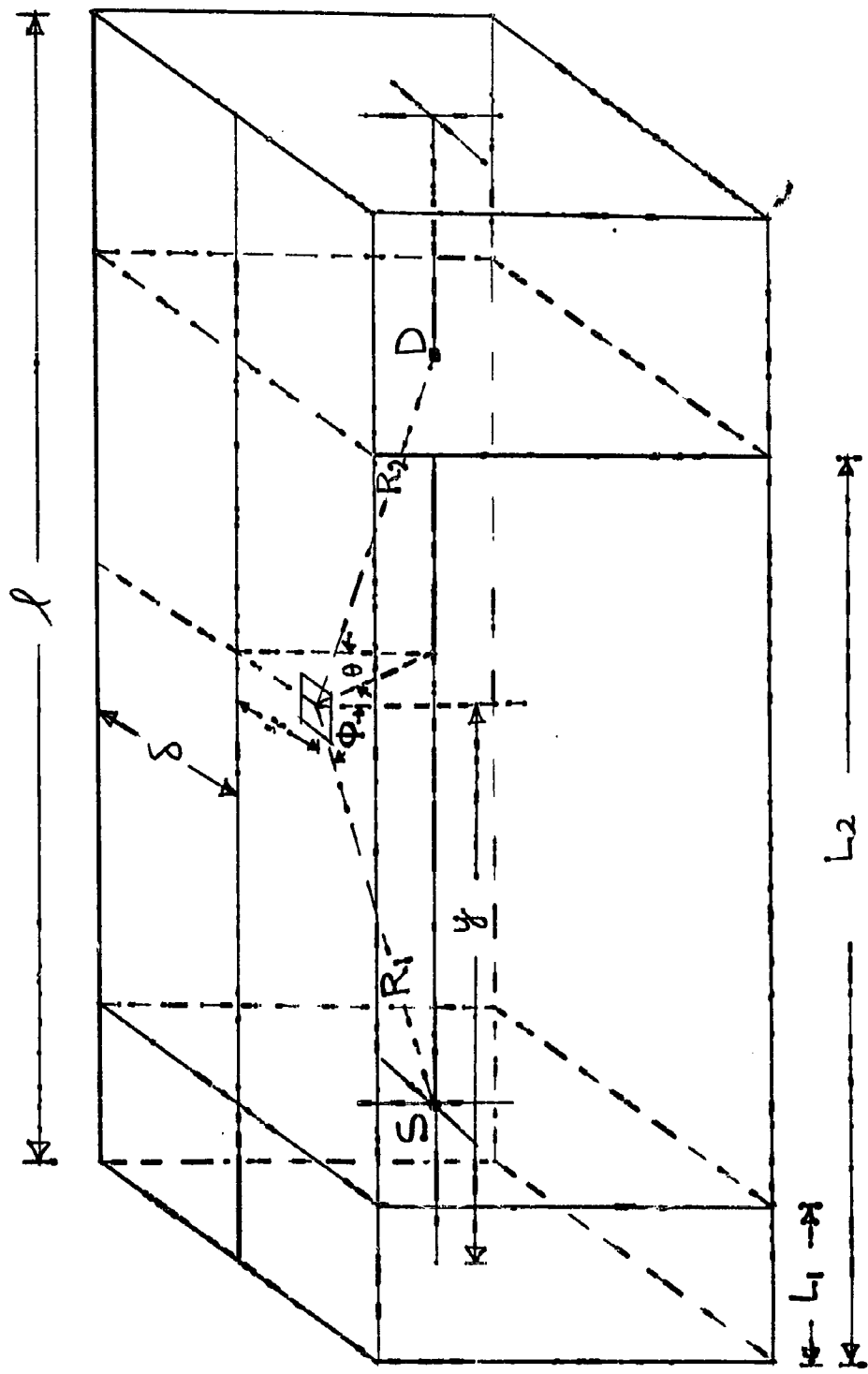


Figure 2. Geometry Used by Computer Program to Calculate Doses and Fluxes in Straight Rectangular Ducts

To include the multiple reflection,  $\alpha'$  should be replaced by<sup>3</sup>

$$\frac{\alpha'}{1 - \alpha' K_c(\delta, l, y)}$$

where

$$K_c = \frac{1}{2\delta} \left[ l + 2\delta - \frac{y^2 + 2\delta^2}{\sqrt{y^2 + 4\delta^2}} - \frac{(l-y)^2 + 2\delta^2}{\sqrt{(l-y)^2 + 4\delta^2}} \right]$$

The total reflection contribution from the whole duct surface area to the detector is:

$$\phi_c = \frac{kS_o}{\pi^2} \int_{x=0}^l \int_{\theta=0}^{\pi/4} \frac{2\delta A \alpha'}{(1 - K_c \alpha') R_2} \frac{\delta^2 \sec^2 \theta d\theta dy}{R_1^3 R_2^2}$$

## 2. Isotropic Re-emission Distribution

For this case the reflection contribution from an element area  $dA'$  at  $(y, \delta, 0)$  is

$$\frac{kS_o}{4\pi} \times \frac{1}{R_1^2} \times \frac{\delta}{R_1} \times \alpha'(E, \theta) \times B \times \frac{1}{2\pi R_2^2} \times dA'$$

<sup>3</sup> Simon, A. and C. E. Clifford, "The Attenuation of Neutrons by Air Ducts in Shields," Nuc. Sci. and Engr. 1, 156-166 (1956).

and the total reflected contribution to the detector is:

$$\phi_I = \frac{kS_0}{\pi^2} \int_0^l \int_0^{\pi/4} \frac{B\alpha'}{(1 - K_I \alpha')} \frac{\delta^2 \sec^2 \theta d\theta dy}{R_1^3 R_2^2}$$

where B is the fraction of the total re-emission distribution which is isotropic, and  $B = 1 - A$ .

$$K_I = \frac{1}{2} \left[ \frac{(l-y)}{\sqrt{(l-y)^2 + 4\delta^2}} \left\{ 1 + \frac{1}{4} \frac{4\delta^2}{(l-y)^2 + 4\delta^2} + \frac{9}{64} \frac{16\delta^4}{[(l-y)^2 + 4\delta^2]^2} \right\} + \frac{y}{\sqrt{y^2 + 4\delta^2}} \left\{ 1 + \frac{1}{4} \frac{4\delta^2}{y^2 + 4\delta^2} + \frac{9}{64} \frac{16\delta^2}{[y^2 + 4\delta^2]^2} \right\} \right]$$

where only the first three terms have been retained. Here, both  $K_c$  and  $K_I$  are derived for cylindrical geometry with the Simon and Clifford assumption that the multiple reflection integrand dominates for the radiation scattered points in a plane perpendicular to  $l$  at  $y$ . It is also assumed that these functions are not very sensitive to the difference between rectangular and cylindrical geometry and so they are used with a radius equal to the half width of the duct. In addition it is assumed that they are also not sensitive to the position of the source and the detector.

The total flux seen by the detector is the direct plus the reflected contributions

$$\phi_T = \frac{kS_o}{4\pi(L_2-L_1)^2} + \frac{kS_o}{\pi^2} \int_{y=0}^l \int_{\theta=0}^{\pi/4} \left[ \frac{2\delta A}{(1-K_c a')R_2} + \frac{(1-A)}{(1-K_1 a')} \right] \frac{a'^2 \sec^2 \theta d\theta dy}{R_1^2 R_2^2}$$

### C. Albedo Data

#### 1. Gamma Rays

Monte Carlo calculated gamma ray albedo values for incident angles ranging from 0° to 90° and for energies from 0.2 mev to 2 mev were fitted to a simple expression. For concrete, the expression is:

$$a'(\theta) = a e^{-b \cos \theta} + c \cos \theta$$

Best fit to gamma and neutron incident (III-C-1) angle dependence.

where  $\theta$  is the incident angle and a, b and c are parameters to be evaluated for the given gamma ray or neutron source energy.

From the referenced report<sup>2</sup>, little information about the re-emission distribution is available. Where the cosine and isotropic re-emission distributions dominate, for perpendicular and grazing incidence respectively, the distribution is found to be an approximate fit to the following:

$$A(\theta) = \sqrt{\cos \theta}$$

(III-C-2)

Best fit to gamma  
re-emission data

$$B(\theta) = 1 - \sqrt{\cos \theta}$$

(III-C-3)

where A and B represent the cosine and isotropic re-emission distribution parts respectively. It is assumed that the albedos for other materials will behave in a similar way as concrete.

## 2. Neutrons

Little incident angle dependence data for neutrons is available. Equation III-C-1 may be used for any desired incident angle dependence or if in equation III-C-1,  $b = c = 0$ , then  $a' = a$  and the albedo is constant for all incident angles.

For re-emission distributions, again either isotropic or cosine dependence should be used until dependences such as equations III-C-2 and III-C-3 for gamma rays have been determined.

## D. Programming Notes

The following are included to aid users of the computer program.

1.  $x$  is measured from the centerline of the duct.
2.  $y, L_1$  and  $L_2$  are measured from the duct entrance.
3. All source and detector positions are on the centerline.
4. The program assumed symmetry about the centerline for the four faces and for the two halves of any face.

5. This program will work directly for a square cross section tunnel, and with a simple modification for other cross sections.
6. No approximation based on  $\frac{\delta}{\ell} \ll 1$  is used.
7. This program can be used for a circular cross section duct of radius  $\delta$  by integration along  $y$  (let  $\theta_0 = 0$ ,  $\theta_n = \frac{\pi}{4N}$   $\ll$   $\frac{\pi}{4}$  and  $n = 4$ ) and by multiplying the reflection contribution part by  $N^2$ . (See input data)

E. Code Input Data

The following are the input data symbols necessary for all cases that this program can handle, expressed in IT (Univac) and Fortran (IBM) program language:

<u>Fortran</u>	<u>IT</u>	
D <sub>1</sub>	I1	n: number of increments of $\theta$ to be integrated over but where n is always taken as an even number.
D <sub>4</sub>	I4	N: number of increments of $y$ to be integrated over but where N is always taken as an even number.
Y202	Y201	$\theta_0$ : the initial value of $\theta$ expressed in radians.
Y203	Y202	$\theta_n$ : the final value of $\theta$ expressed in radians.
Y204	Y203	$y_0$ : the initial value of $y$ .
Y205	Y204	$y_n$ : the final value of $y$ .
Y206	Y205	$\frac{kS_0}{2\pi}$ : where $kS_0$ is the source strength expressed in R/hr.
Y207	Y206	$\ell$ : the total length of the duct.
Y208	Y207	$\delta$ : the half width of the duct.
Y209	Y208	$L_1$ : the source distance from the entrance end of the duct.

FortranIT

Y210	Y209	$L_2$ :	the detector distance from the entrance end of the duct.
Y211	Y210	a:	a parameter for the albedo expression.
Y212	Y211	b:	a parameter for the albedo expression.
Y213	Y212	c:	a parameter for the albedo expression.
Y500	C499	g:	a parameter designed to be 0, 1 and 2 for an isotropic, cosine or both, distributions respectively.

Other symbols used in the IT program are listed below in the order that they appear in the program.

Y216	$\Delta\theta$
Y224	$\delta^2$
Y225	$\rho^2$
Y226	$L_1^2$
Y227	$L_2^2$
Y228	$R_1(\theta = 0, y = 0)$
Y229	$R_2(\theta = 0, y = 0)$
Y230	$\cos \theta (\theta = 0, y = 0)$
C408	$\alpha'(\theta = 0, y = 0)$
Y231	$\theta_D$
Y221	$y_i$
I5	the y subscript i, $i \leq 700$
I3	the initial value for i or j

Y217	$\theta_j$
I2	the $\theta$ subscript $j$ , $j \leq 700$
C401	$\delta^2 \sec^2 \theta$
C402	$R_1$
C403	$\cos \theta$
C404	$\alpha'$
C405	$K_1'$ (first part of the $K_1$ expression)
Y218	$S_1$ for $\theta$ (summation by Simpson rule)
Y202	$\Delta y$
C501	$\phi_R$ ( $y = 0$ )
Y222	$S_1$ for $y$
Y223	$\phi_R$
Y232	$\phi_T$

#### F. Sample Problem

For demonstration as well as checking how and what the code does, a test problem was prepared, and a hand calculation performed as a check. The sample problem is to calculate the gamma dose rate at a centerline distance of 6 feet from the entrance of a 6 by 6 foot, 18 foot long straight concrete duct. A 0.2 mev source of strength  $kS_0$ , such that  $kS_0/\pi^2 = 1$  was chosen, and the source is positioned 3 feet from the entrance. The albedo parameters  $a$ ,  $b$ , and  $c$  were fitted to the NBS data and found to be 0.48, 2.0, and 0.08, respectively. A cosine as well as an

isotropic re-emission distribution was expected, in which case  $g = 2$ .

(See previous Section.) Integration over 7 points (6 increments,  $\Delta\theta$ ) and 11 points (10 increments,  $\Delta y$ ) along the length of the duct are chosen. The input data needed is as follows:

$n = 6$	$y_N = 18$ feet	$L_2 = 6$ feet
$N = 10$	$kS_0/\pi^2 = 1$ R/hr $\times$ ft <sup>2</sup>	$a = 0.48$
$\theta_0 = 0$ radians	$l = 18$ feet	$b = 0.2$
$\theta_n = 0.7854$ radians	$\delta = 3$ feet	$c = 0.08$
$y_0 = 0$ feet	$L_1 = 3$ feet	$g = 2$

The code "unconditional" output will appear as follows:

$\phi_T = 0.1072509$ R/hr	$y_0 = 0$ feet	$y_N = 18$ feet	$\phi_R = 0.019984$ R/hr
$a = 0.48$	$b = 2.0$	$c = 0.08$	$\frac{kS_0}{\pi^2} = 1$

Values of many of the intermediate steps of the calculation may be printed out if "conditional" output is called for.

We note that the code gave a detector reading of  $\phi_T = 0.1072$  R/hr of which the reflected contribution ( $\phi_R = 0.01998$  R/hr) is approximately 19% of the total.

A hand calculation was performed to insure the correctness of the computer program.

The IT and Fortran programs are given in Appendix IV. The Fortran program was translated directly from the IT program but was not run.

#### IV. EXPERIMENTAL PROGRAM

From the beginning of the Radiation Streaming program the dominant philosophy which has guided the experimental planning has been to design experiments and perform measurements which will be amenable to theoretical treatment. Because of the simplicity of albedo theory we have persisted in the contention that the albedo formalism will more than adequately do the job of giving the designer a tool to determine the radiation attenuation of a duct.

Because of the importance to the military (hardened bases) and to the civil defense requirements (personnel shelters), this program has to date, layed major emphasis on large ducts and entranceways.

##### A. Description of Experiments

Figures 3, 4, and 5 show different views of a concrete entranceway having a single 90° bend. The width and height of the duct are 6 feet with 1 foot thick concrete walls except where additional thickness has been added to ensure against radiation leakage between source and detector.

The walls are built from interlocking blocks to avoid cracks.

More details may be seen in Figures 11 through 15 of ARF-1158-12.

##### B. Gamma Dose Rate Distribution Measurements

As the previous program had investigated Co-60 ( $\bar{E} = 1.25$  mev) and Cs-137 (0.67 mev) dose rate distributions in the 6 by 6 foot duct, we wished to extend the studies to higher and lower photon energies. For this purpose Na-24 (2.76 mev and 1.36 mev) and Au-198 (0.411 mev) sources were used.

ARMOUR RESEARCH FOUNDATION OF ILLINOIS INSTITUTE OF TECHNOLOGY

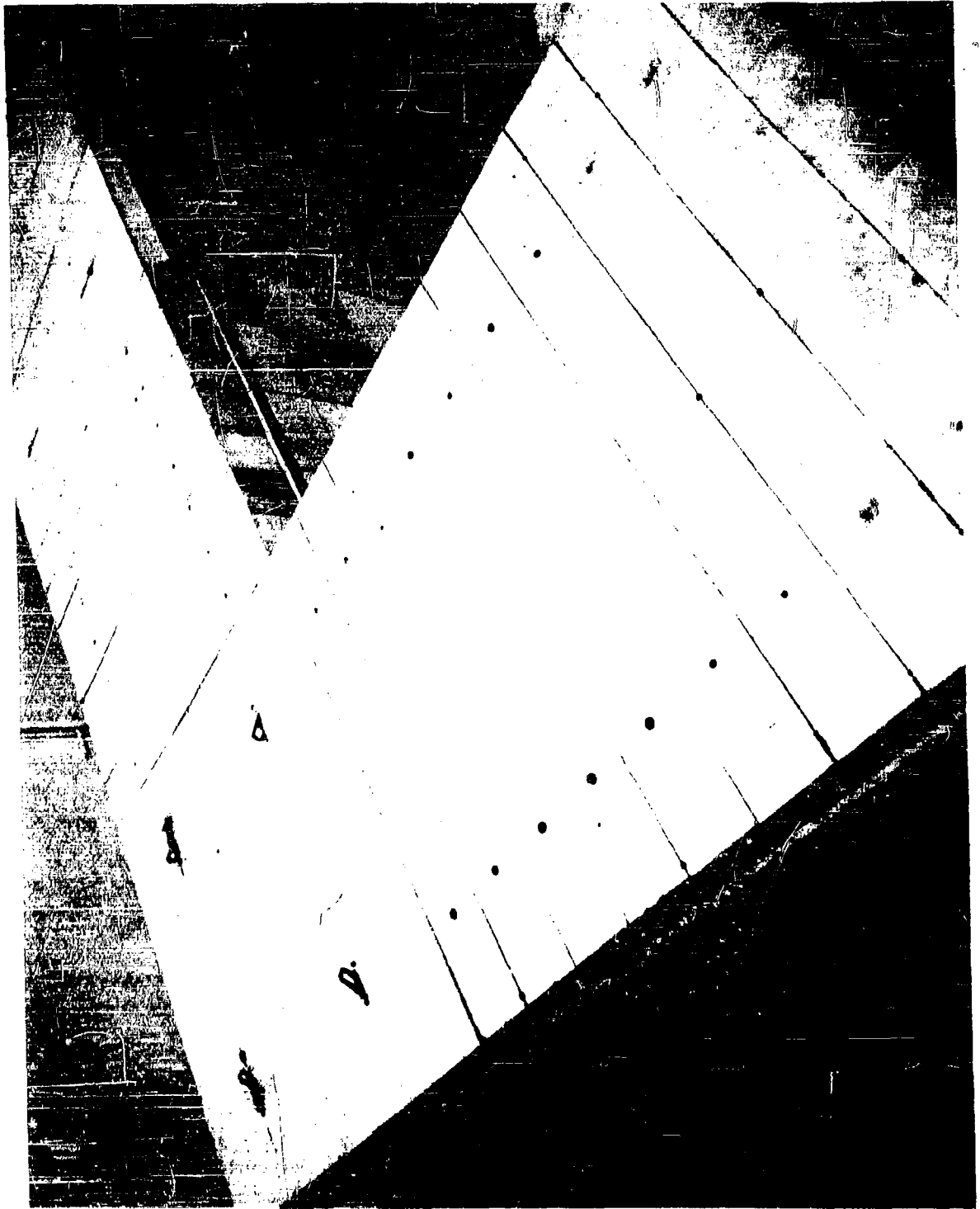


Figure 3. Assembled Concrete Entranceway

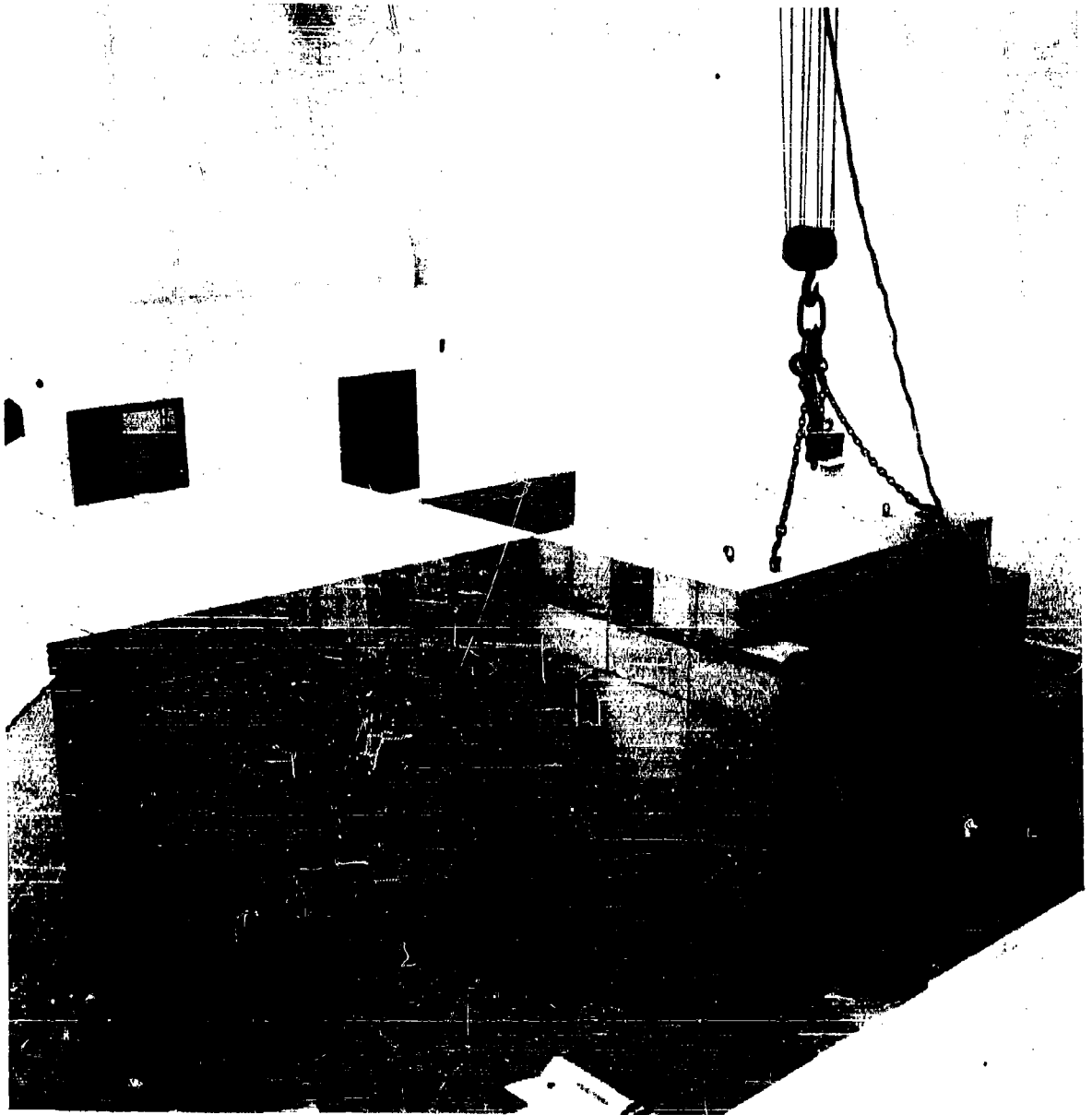


Figure 4. Concrete Entranceway with Roof Section Removed

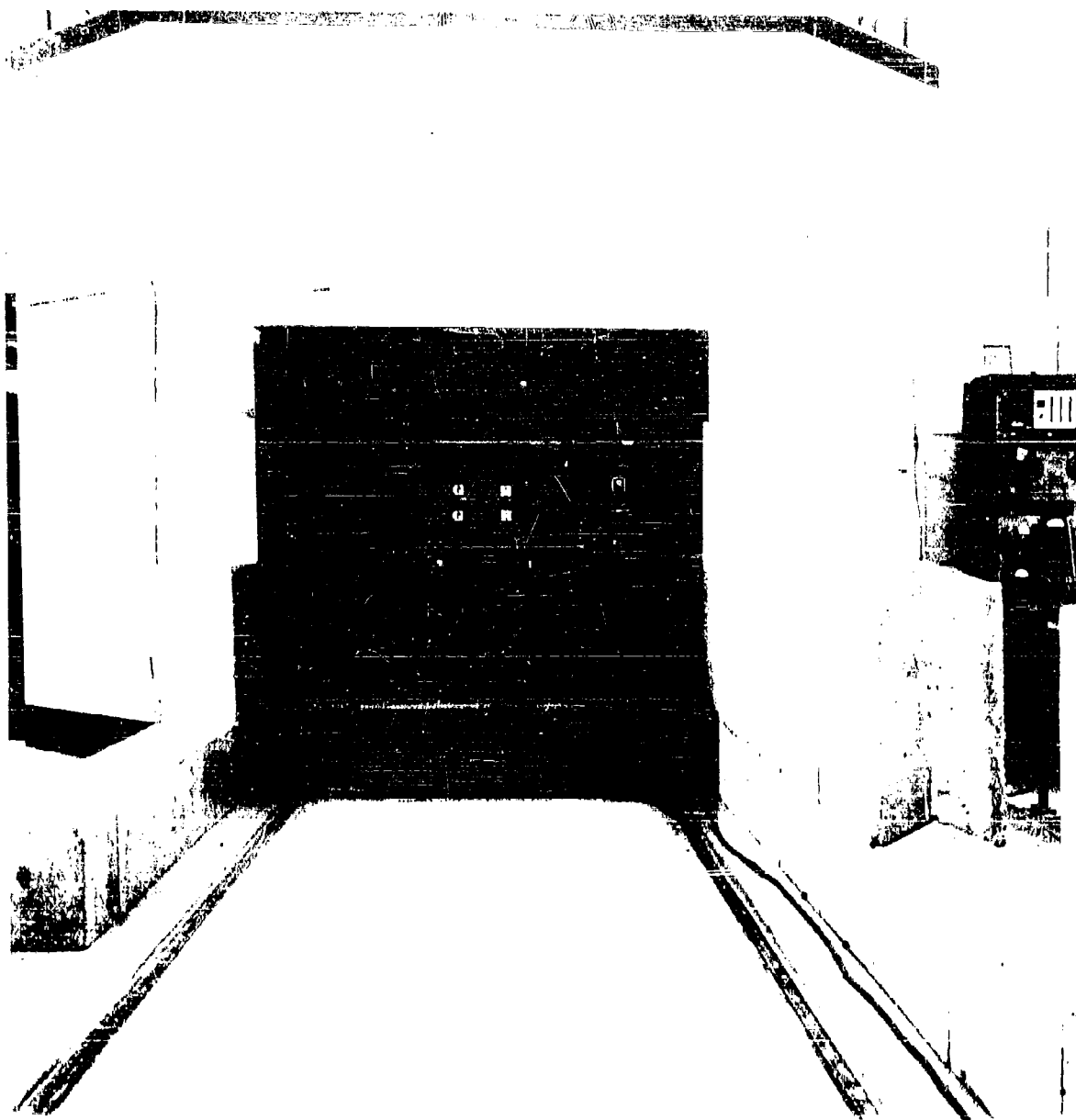


Figure 3. Concrete airway, Partially Assembled

## 1. Sources

The gold source was prepared in the form of a cylinder, one (1) inch in diameter and six (6) inches long. The gold cylinder wall thickness was 0.01 inches to minimize photon self absorption and scattering. The gold cylinder was slipped into a thin walled (0.017 inch) aluminum can of slightly larger dimensions and aluminum solder sealed. Such permanent construction allows the source to be reactivated at any time in the future. A five hour irradiation of the 19.2 gram gold source resulted in an estimated 8.1 curies of activity at shutdown. Study of the Au-198 decay scheme indicates that 99 out of every 100 disintegrations produces the desired 411 kev photon.

The sodium source was made as follows: NaF, packed to a measured density of  $1.67 \text{ g/cm}^3$  by a high pressure press, was contained in an aluminum can and sealed. The active length of the NaF was 6 inches and of 7/8 inch diameter. The aluminum can contained a total of 54.1 grams of Na.

Na-24 has a decay scheme like Co-60 in that a pair of cascade gammas result from each disintegration ( $E_1 = 2.76 \text{ mev}$  and  $E_2 = 1.37 \text{ mev}$ ). In order to be sure that self absorption was not modifying the spectrum, the source was given a one minute activation in the Armour Research Reactor. One hour was allowed to be certain that the 2.3 minute aluminum activity had decayed. The Na-24 source was then placed 1 meter from a 3 x 3 inch NaI crystal and on axis and the spectrum swept out with a

256 channel analyzer. The spectrum observed was found to be a perfect Na-24 spectrum.

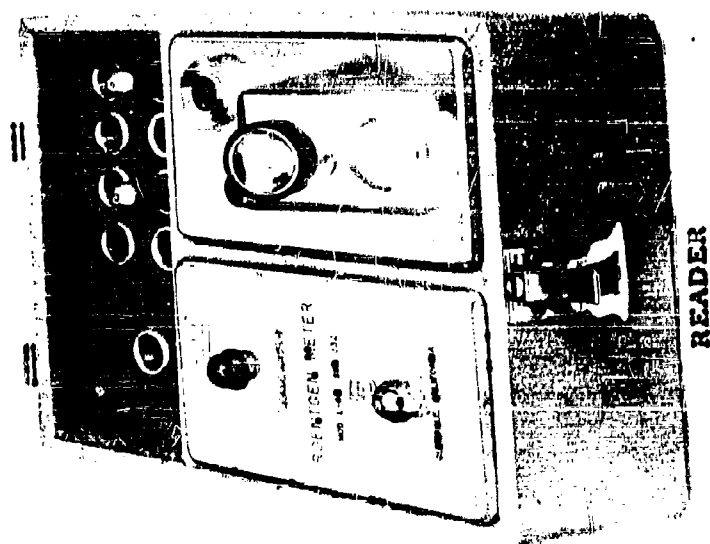
A twelve hour irradiation of the 54.1 gram sodium source in the central exposure tube of the Armour Research Reactor produced approximately 7.4 curies of Na activity. Fifteen hours of decay was allowed so that known impurities in the aluminum container were decayed out. When the measurements started the source strength was approximately 4.2 curies.

The source, in all cases to be reported, is located in the exact geometrical center of the duct, being raised by a pulley system from a moveable pig on the floor of the duct. Detector exposure times were measured with a stop watch.

## 2. Detectors

As for all previous work, the Landsverk ionization chambers were again used for all dose measurements. Three-sixteenth (3/16) inch thick bakelite sleeves, provided by Landsverk, were used for all measurements. The sleeves were modified so as to cover the top of the chambers as well.

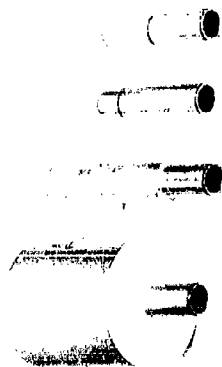
No energy dependence measurements were made. We assumed the chamber's response to be linear up to 2.76 mev. Figure 6 is a photograph of the chambers employed, including the neutron detector ( $\text{BF}_3$ ) and cadmium sleeve discussed later.



Bakelite Sleeves



1 mr



10 mr 100 mr 1 R 10 R



BF 3



Cd Sleeve



Figure 6. Photograph of Detection Equipment.

### 3. Results

#### a. Sodium source measurements

As we wished to extend the study to include the effect of long leg lengths, the 6 by 6 foot concrete entranceway was modified as shown in Figure 7. Here, part of the Reactor's biological shield was used to extend the length of leg  $l_1$ .  $l_1$  is defined as the distance from the source to the beginning of the bend.  $l_2$  is seen to be 16 feet.

Figure 7 shows the three source positions  $S_{14}$ ,  $S_{10}$  and  $S_7$  used. These source positions define three  $l_1$ 's,  $l_1 = 14$ ,  $l_1 = 10$ , and  $l_1 = 7$  feet. The positions labeled A, 1, 1a', 1a, 2, 3, 4, etc., up to 11a are the detector positions at which measurements were made.

Two points about the measured data need explanation.

First, referring to Figure 7, when a measurement is made at, say position 3, that position is characterized as a measurement for which  $l_2 = 8$ . We say the same measurement would be obtained if the remaining 8 feet of the duct behind position 3 were not present. This was established in the first program and is valid for gamma rays only, not neutrons.

Second, sodium has a half life of approximately 15 hours and thus decayed substantially over the week period required to make the measurements. Decay corrections ( $e^{-\lambda t}$ ) were computed for each of the 130 measurements made for the three source positions. The correction was made back to the time of the first measurement (position A) for the first

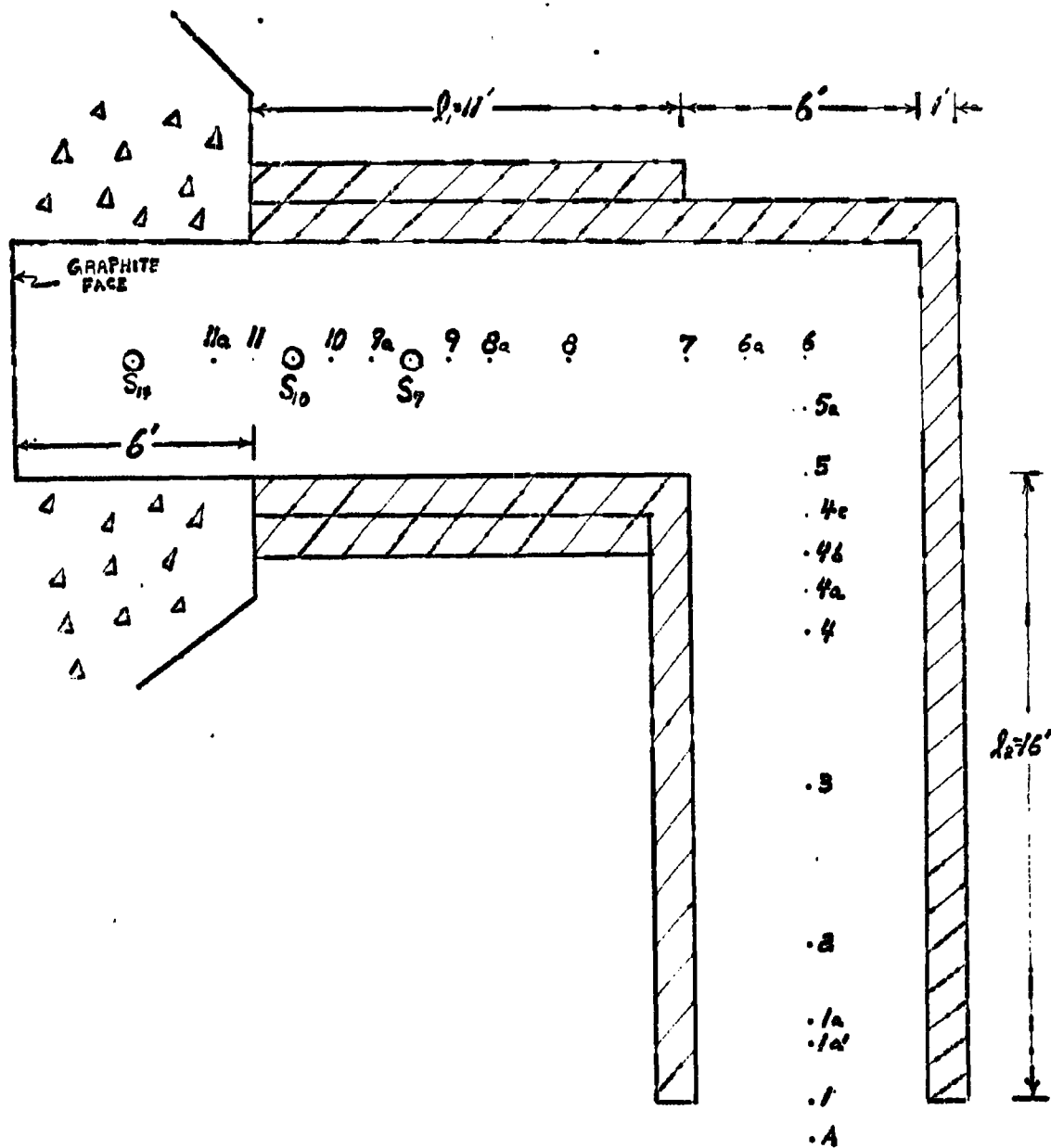


Figure 7. Gamma Dose Rate Distribution Measurements

source position used,  $S_{14}$ . Multiple measurements were made at each detector position and averaged.

The data of Table I are plotted in Figures 8 and 9; the data of Table II, in Figures 10 and 11; and that of Table III in Figures 12 and 13.

Observation of Figures 9, 11, and 13 shows an almost  $1/R^2$  falloff in the first leg. This is quite reasonable in view of the low albedo for sodium energies. Note that for neutrons (Figure 26) the albedo appears to play a more significant role in view of the nearly  $1/R$  falloff.

Of significance is the slope of the second leg ( $l_2$ ) data. If the second leg data are normalized and plotted, all three ( $l_1 = 7, 10, \text{ and } 14$ ) fall on top of each other. Hence, the rate of falloff in the second leg appears to be independent of the length of  $l_1$  for sodium energies.

In Figures 12 and 13 the data point at 27 feet is clearly a bad measurement. A review of the measurement data, however, offers no justification for disregarding the point.

Finally, no error measurements are indicated as the error is less than the height of an error bar that could be drawn. From the experimental point of view the total error in a measurement is probably less than 5%. Only the energy dependence of the detectors at 2.76 mev is in doubt.

TABLE I

Gamma Dose Rate Measurements in 6 by 6 Foot Concrete Entranceway  
 Na-24 Point Source at S<sub>14</sub>

Measurement position	Centerline distance from source (ft)	$h_1$ (ft)	$h_2$ (ft)	Dose rate (mr/min)	Dose* attenuation factor
A	37	14	---	0.0067	822
1	36	14	16	0.0077	715
1a	34	14	14	0.0105	523
2	32	14	12	0.0138	398
3	28	14	8	0.0323	171
4	24	14	4	0.105	52.2
4a	23	14	3	0.164	53.6
4b	22	14	2	0.276	20.0
4c	21	14	1	0.727	7.58
5	20	14	---	5.00	1.10
5a	18.5	14	---	5.46	-----
6	17	14	---	5.51	-----
6a	15.5	14	---	6.65	-----
7	14	14	---	7.91	-----
8	11	14	---	12.4	-----
9	8	14	---	22.2	-----
10	5	14	---	55.1	-----
11	3	14	---	146	-----
11a	2	14	---	300	-----

\*Dose attenuation factor is always defines as ratio of Position No. 6 reading to the position of measurement reading.

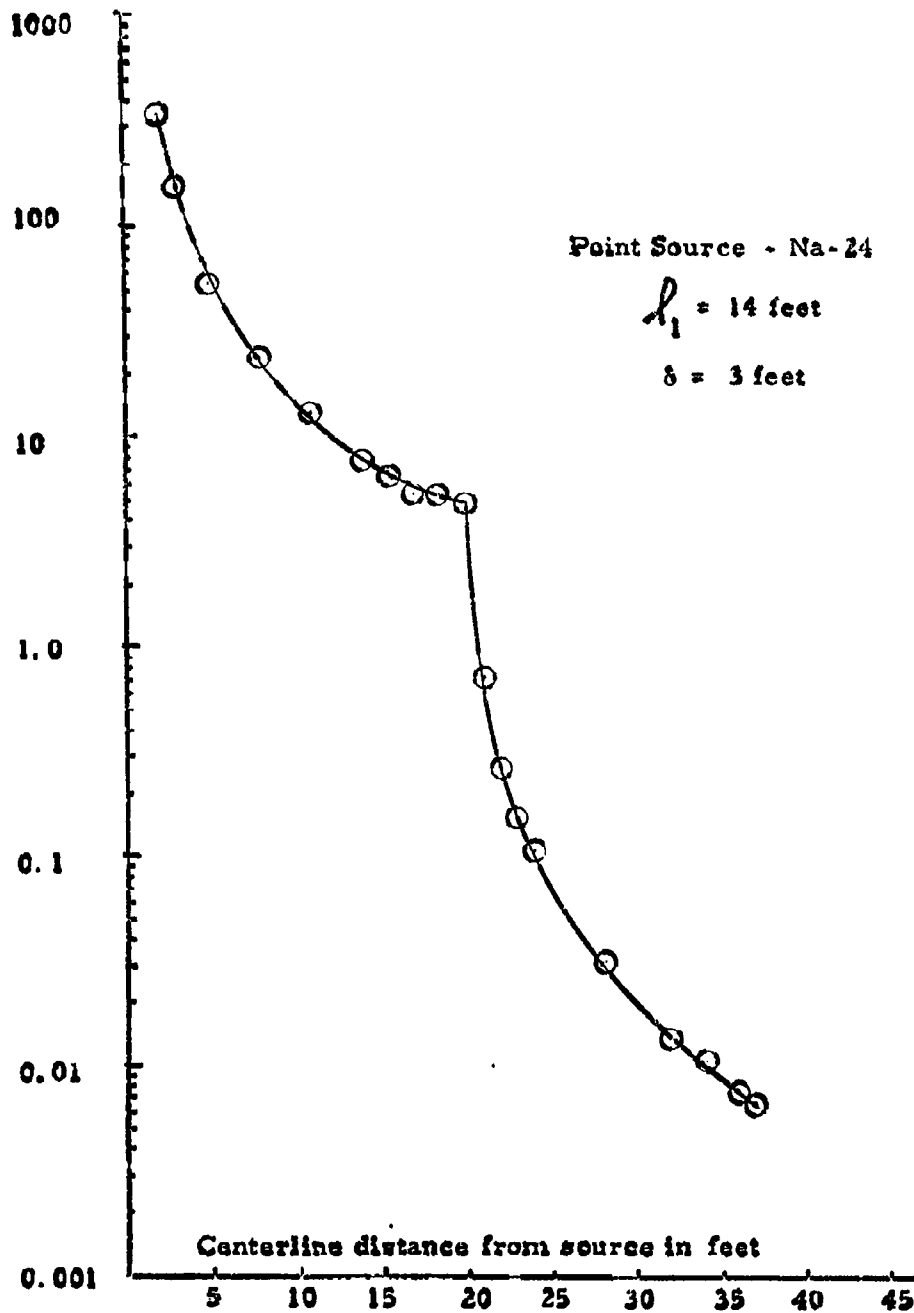


Figure 8. Measured Gamma Dose Rate Centerline Distribution in 6 by 6 Foot Concrete Entranceway with Single Right Angle Bend.

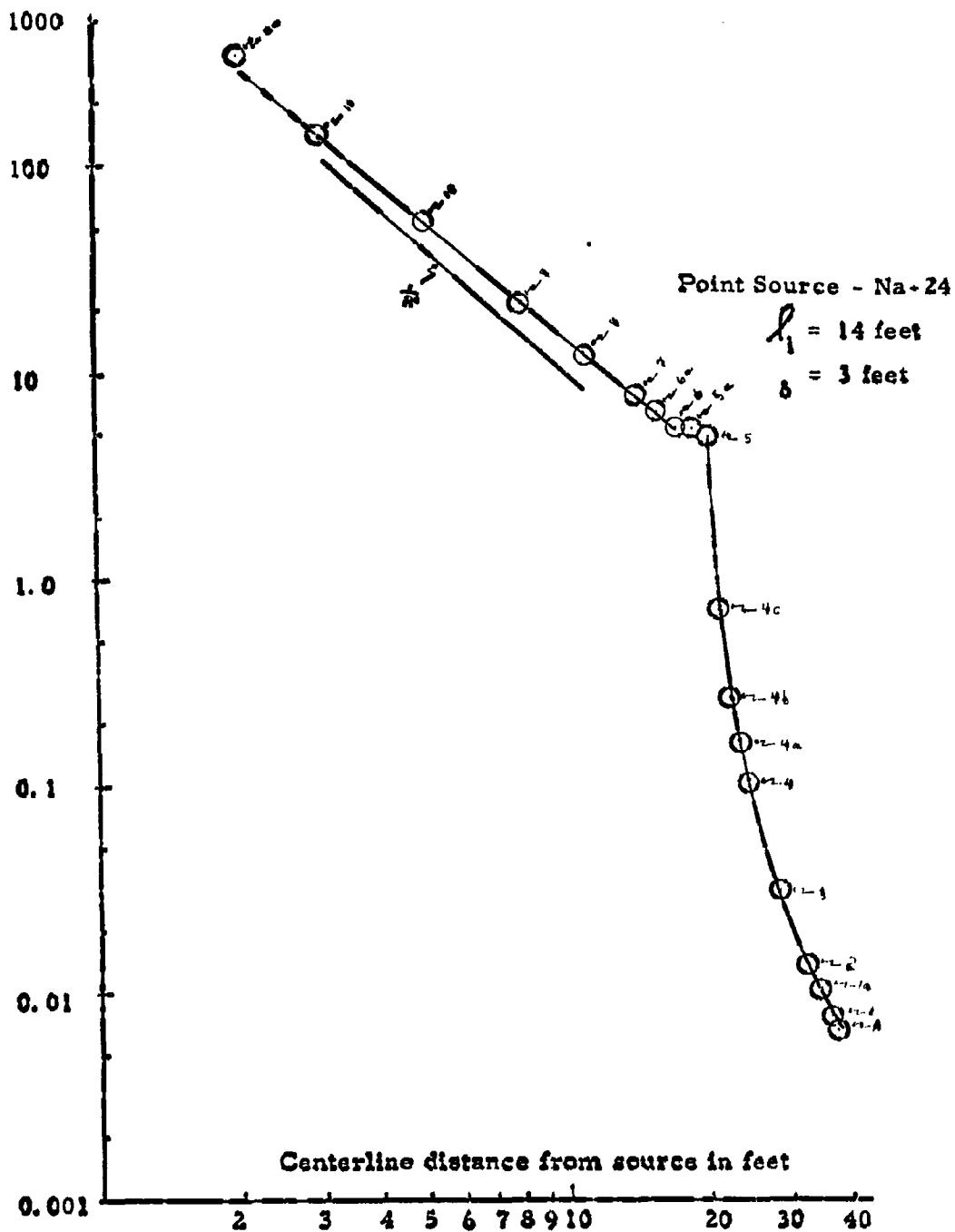


Figure 9. Measured Gamma Dose Rate Centerline Distribution in 6 by 6 Foot Concrete Entranceway with Single Right Angle Bend.

TABLE II

Gamma Dose Rate Measurements in 6 by 6 Foot Concrete Entranceway  
 Na-24 Point Source at  $S_{10}$

Measurement position	Centerline distance from source (ft)	$h_1$ (ft)	$h_2$ (ft)	Dose rate (mr/min)	Dose attenuation factor
1	32	10	16	0.0152	587
1a'	30.5	10	14.5	0.0175	511
2	28	10	12	0.0278	321
3	24	10	8	0.0607	147
4	20	10	4	0.210	42.6
4a	19	10	3	0.330	27.1
4b	18	10	2	0.621	14.4
4c	17	10	1	3.61	2.48
5	16	10	---	8.06	1.11
5a	14.5	10	---	8.83	-----
6	13	10	---	8.95	-----
6a	11.5	10	---	11.4	-----
7	10	10	---	14.4	-----
8	7	10	---	28.6	-----
9	4	10	---	85.1	-----
9a	2	10	---	340	-----
10	1	10	---	1348	-----

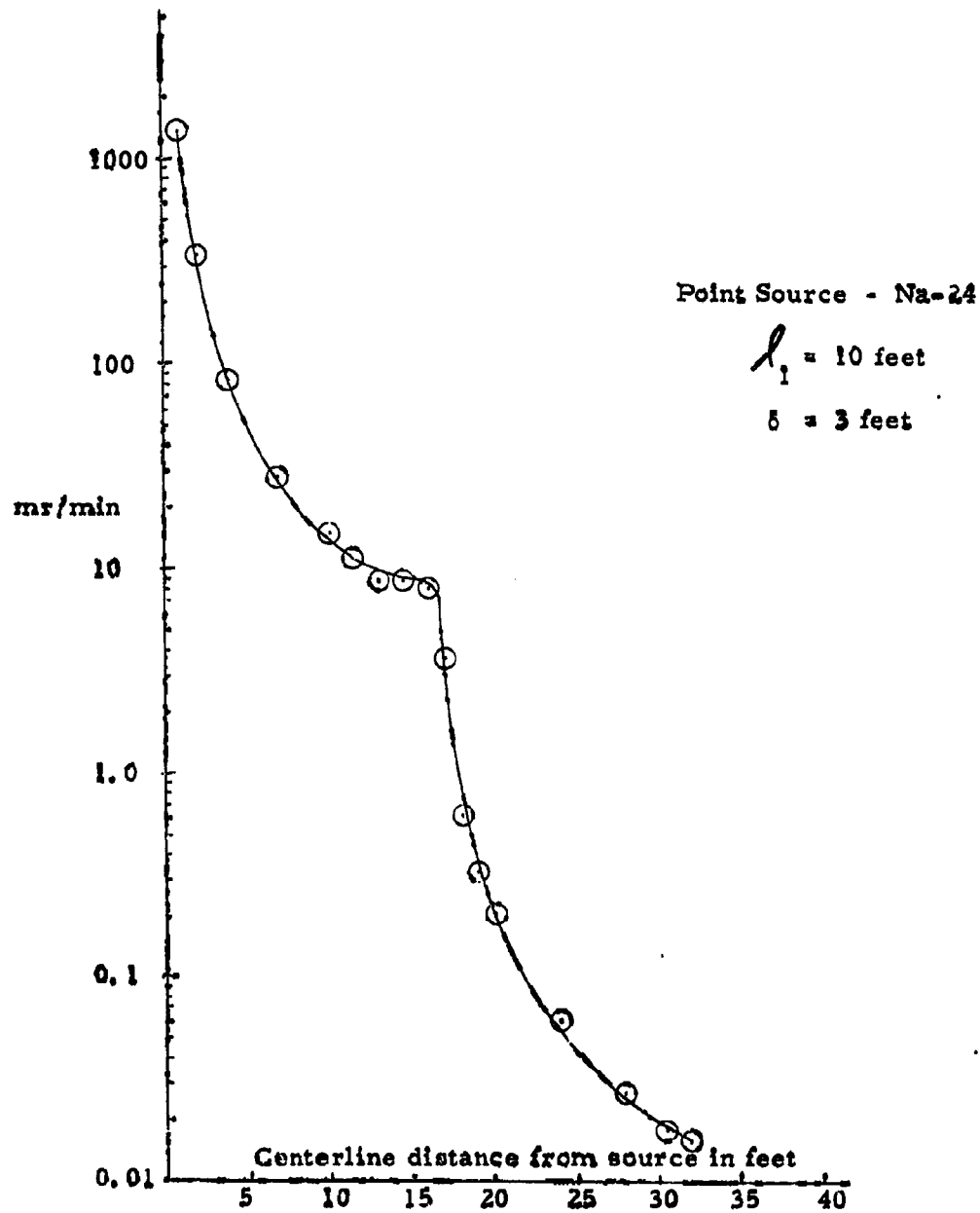


Figure 10. Measured Gamma Dose Rate Centerline Distribution in 6 by 6 Foot Concrete Entranceway with Single Right Angle Bend.

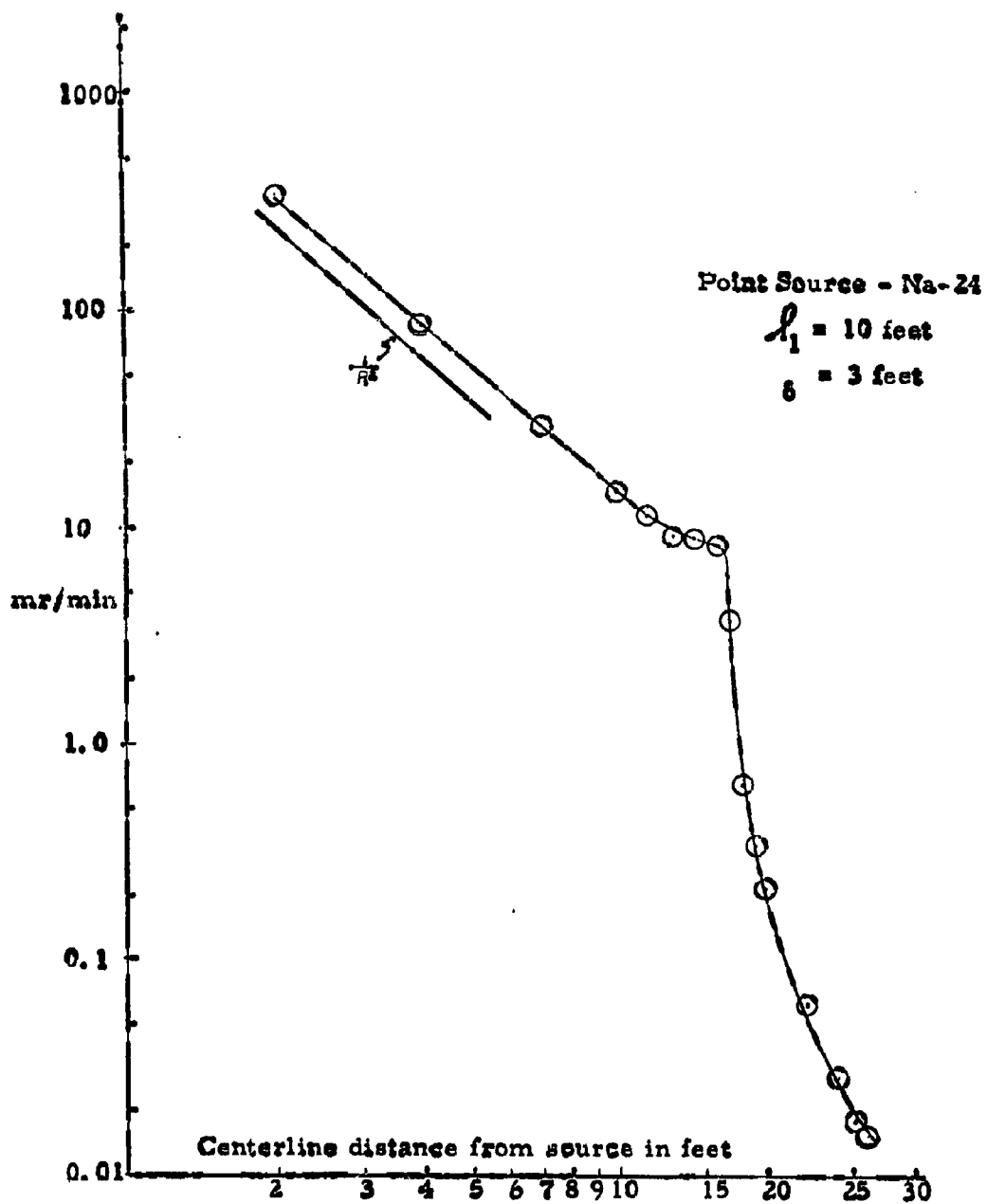


Figure 11. Measured Gamma Dose Rate Centerline Distribution in 6 by 6 Foot Concrete Entranceway with Single Right Angle Bend.

TABLE III

Gamma Dose Rate Measurements in 6 by 6 Foot Concrete Entranceway  
Na-24 Point Source at  $S_7$

Measurement position	Centerline distance from source (ft)	$h_1$ (ft)	$h_2$ (ft)	Dose rate (mr/min)	Dose attenuation factor
1	29	7	16	0.0250	588
1a	27	7	14	0.0409	359
2	25	7	12	0.0467	314
3	21	7	8	0.113	130
4	17	7	4	0.423	34.8
4a	16	7	3	0.661	22.3
4b	15	7	2	1.42	10.3
4c	14	7	1	11.8	1.3
5	13	7	---	12.9	1.13
5a	11.5	7	---	14.2	-----
6	10	7	---	14.7	-----
6a	8.5	7	---	19.8	-----
7	7	7	---	28.3	-----
8	4	7	---	83.6	-----
8a	2	7	---	340	-----
9	1	7	---	1322	-----

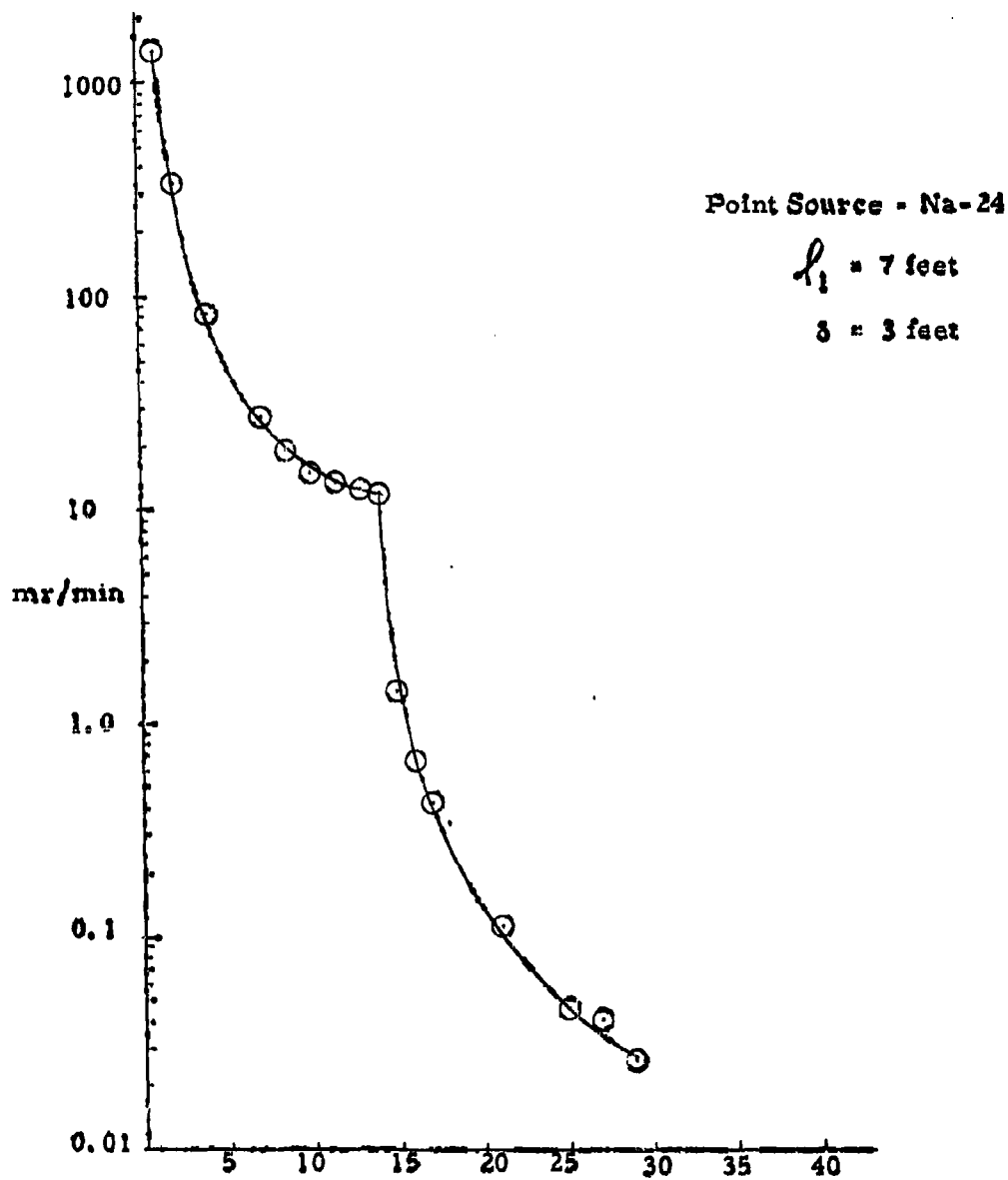


Figure 12. Measured Gamma Dose Rate Centerline Distribution in 6 by 6 Foot Concrete Entranceway with Single Right Angle Bend.

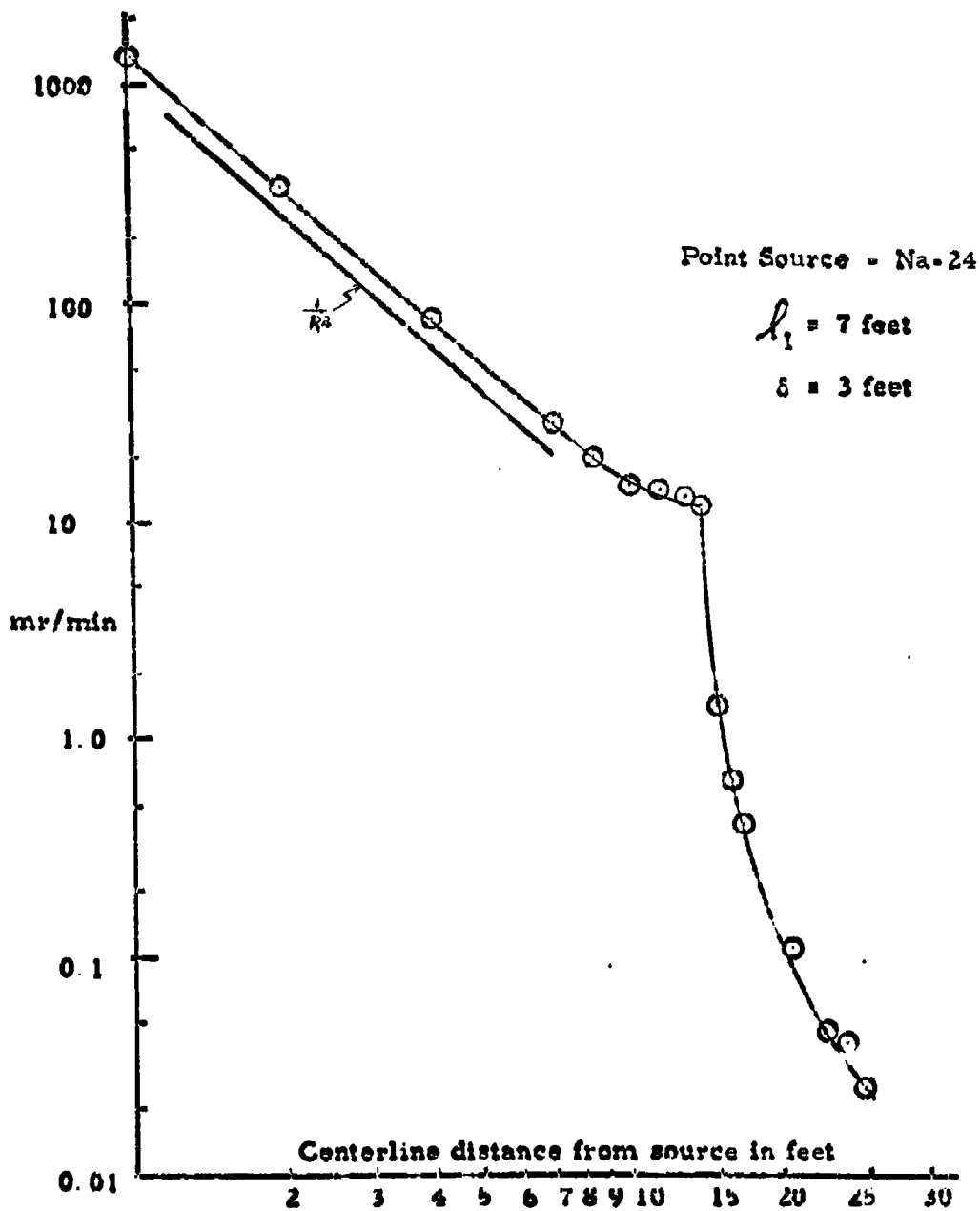


Figure 13 Measured Gamma Dose Rate Centerline Distribution in 6 by 6 Foot Concrete Entranceway with Single Right Angle Bend

#### b. Gold Source Measurements

The use of Au-198 (0.411 mev) as a source was extended to extend the dose rate distribution and dose attenuation factor studies to lower energies. The albedo for gamma rays is known to have an extreme energy dependence.

Measurements made with Au-198 are given in Tables IV, V, and VI, and the data are plotted in Figures 14 through 19. Again, because of the decay of the source ( $t_{1/2} = 2.7$  days) all data is corrected for decay back to the time of the first measurement. (Position No. 1,  $h_1 = 14$ ). In Figure 14, the point at 17 feet is again a bad data point but must be retained.

Study of Figures 15, 17, and 19, again show that the dose rate distribution function in the first leg falls off like  $1/R^2$  just as the much higher energy sodium does. Comparison of the data in Tables III and VI for positions 7 and 8 shows that for sodium (Table III) the dose rate falls off 3.5% less than  $1/R^2$  while for gold the dose rate falls off 7% less than  $1/R^2$ . The difference between the albedos for say 2 mev (sodium average) and 0.4 mev, would give the factor of two difference depending on the angle of incidence chosen.

#### 4. Analysis and Comparison

In an attempt to show trends as the parameters, such as  $h_1$ , and  $h_2$ , and energy vary, Table VII summarizes the dose attenuation ratios. Some pertinent observations are:

TABLE IV

Gamma Dose Rate Measurement in 6 by 6 Foot Concrete Entranceway  
 Au-198 Point Source at S<sub>14</sub>

Measurement position	Centerline distance from source (ft)	$h_1$ (ft)	$h_2$ (ft)	Dose rate (mr/min)	Dose attenuation factor
1	36	14	16	0.00313	301
1a	34	14	14	0.00413	228
2	32	14	12	0.00597	157
3	28	14	8	0.0143	65.7
4	24	14	4	0.0453	20.8
4a	23	14	3	0.0646	14.5
4b	22	14	2	0.101	9.3
4c	21	14	1	0.185	5.1
5	20	14	---	0.990*	-----
6	17	14	---	0.940*	-----
7	14	14	---	1.62	-----
8	11	14	---	2.68	-----
9	8	14	---	4.72	-----
10	5	14	---	10.7	-----
11a	2	14	---	67.1	-----

\* Average of 4 readings.

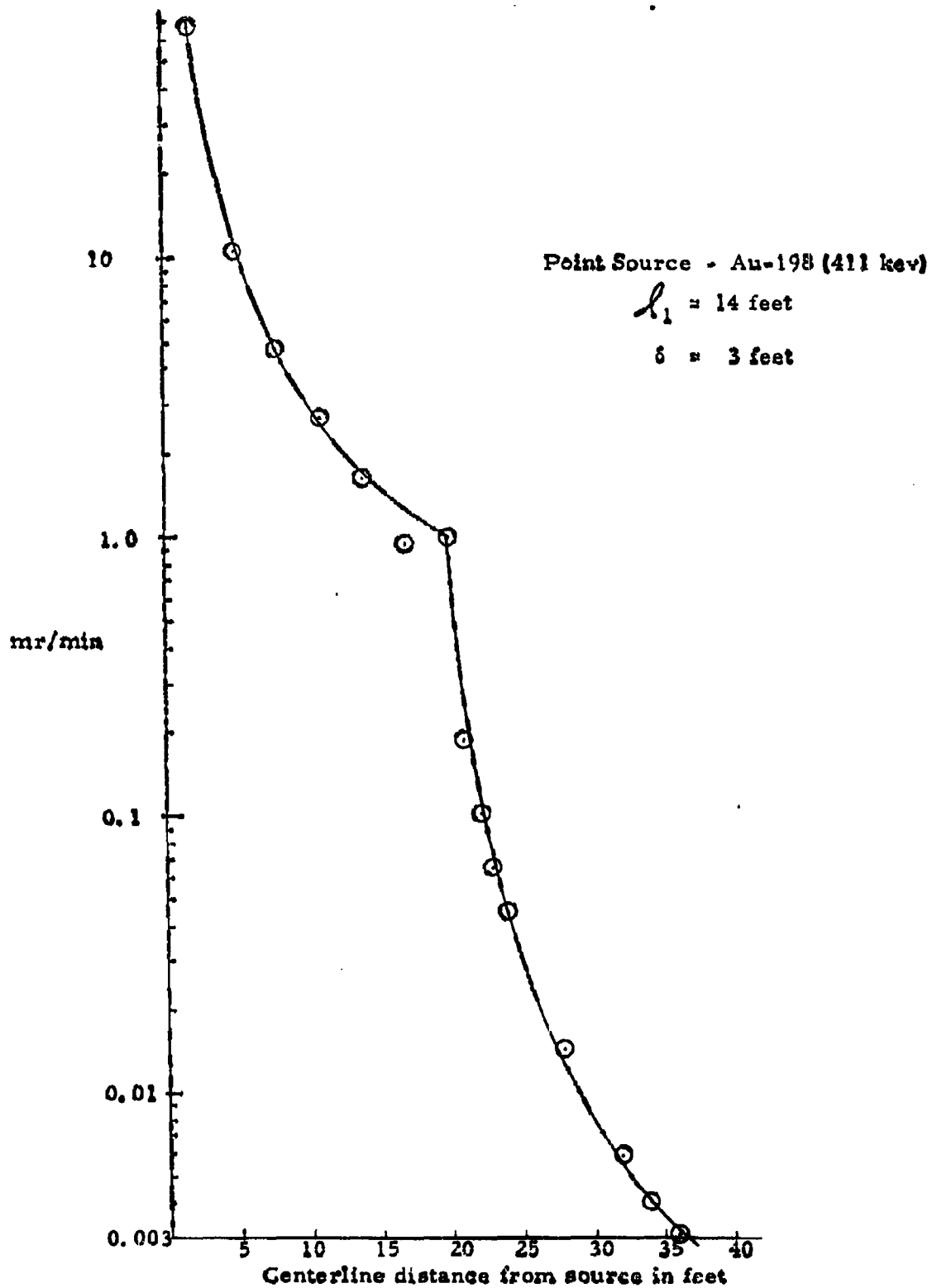


Figure 14. Measured Gamma Dose Rate Centerline Distribution in 6 by 6 Foot Concrete Entranceway with Single Right Angle Bend

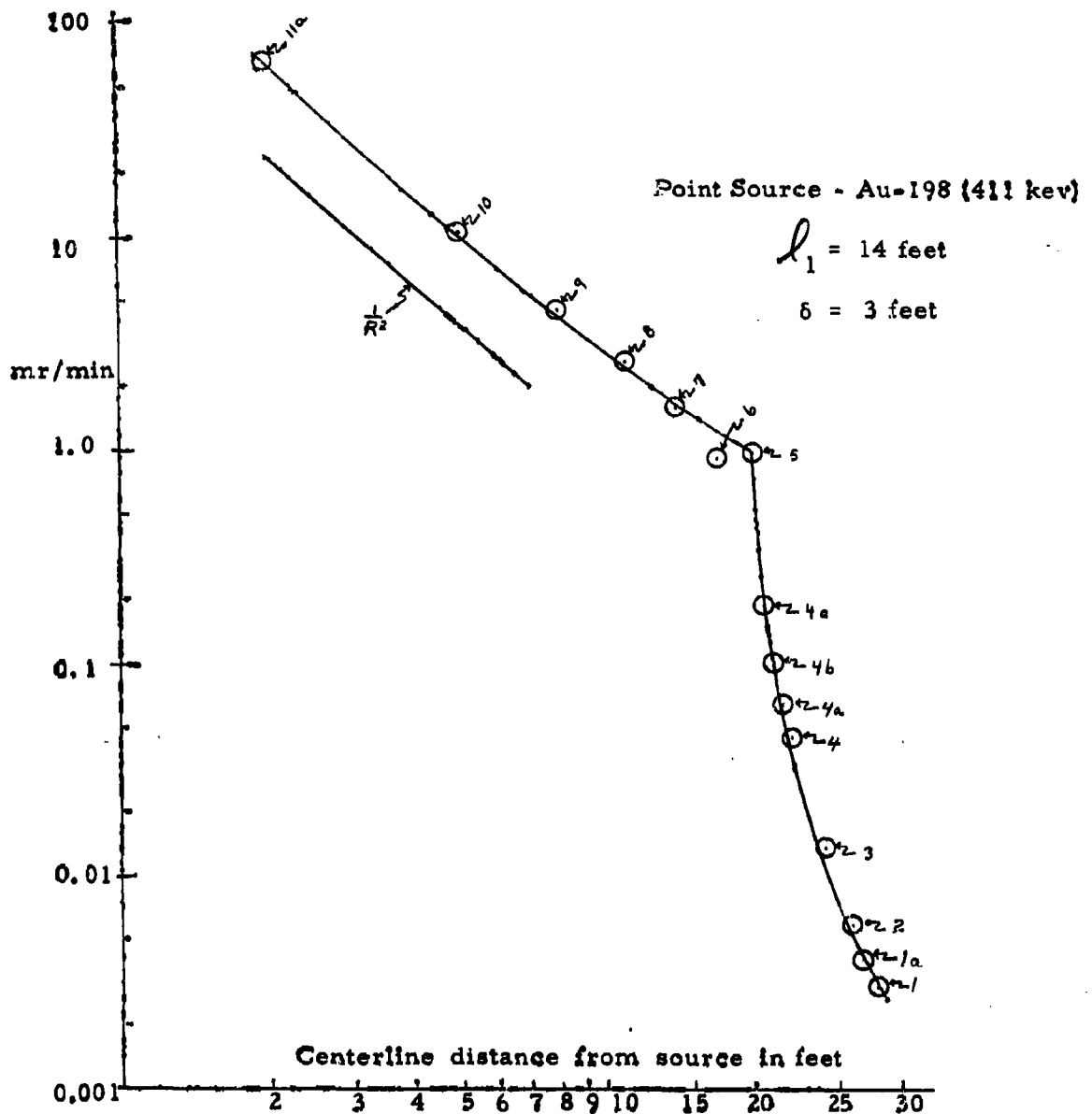


Figure 15. Measured Gamma Dose Rate Centerline Distribution in 6 by 6 Foot Concrete Entranceway with Single Right Angle Bend

TABLE V

Gamma Dose Rate Measurement in 6 by 6 Foot Concrete Entranceway  
 Au-198 Point Source at  $S_{10}$

Measurement position	Centerline distance from source (ft)	$l_1$ (ft)	$l_2$ (ft)	Dose rate (mr/min)	Dose attenuation factor
1	32	10	16	0.00616	303
1a	30	10	14	0.00934	200
2	28	10	12	0.0119	157
3	24	10	8	0.0277	67.9
4	20	10	4	0.0866	21.6
4a	19	10	3	0.150	12.5
4b	18	10	2	0.227	8.23
4c	17	10	1	0.596	3.14
5	16	10	--	1.62	1.15
6	13	10	--	1.87	-----
7	10	10	--	3.04	-----
8	7	10	--	3.83	-----
9	4	10	--	15.4	-----
9a	2	10	--	67.7	-----

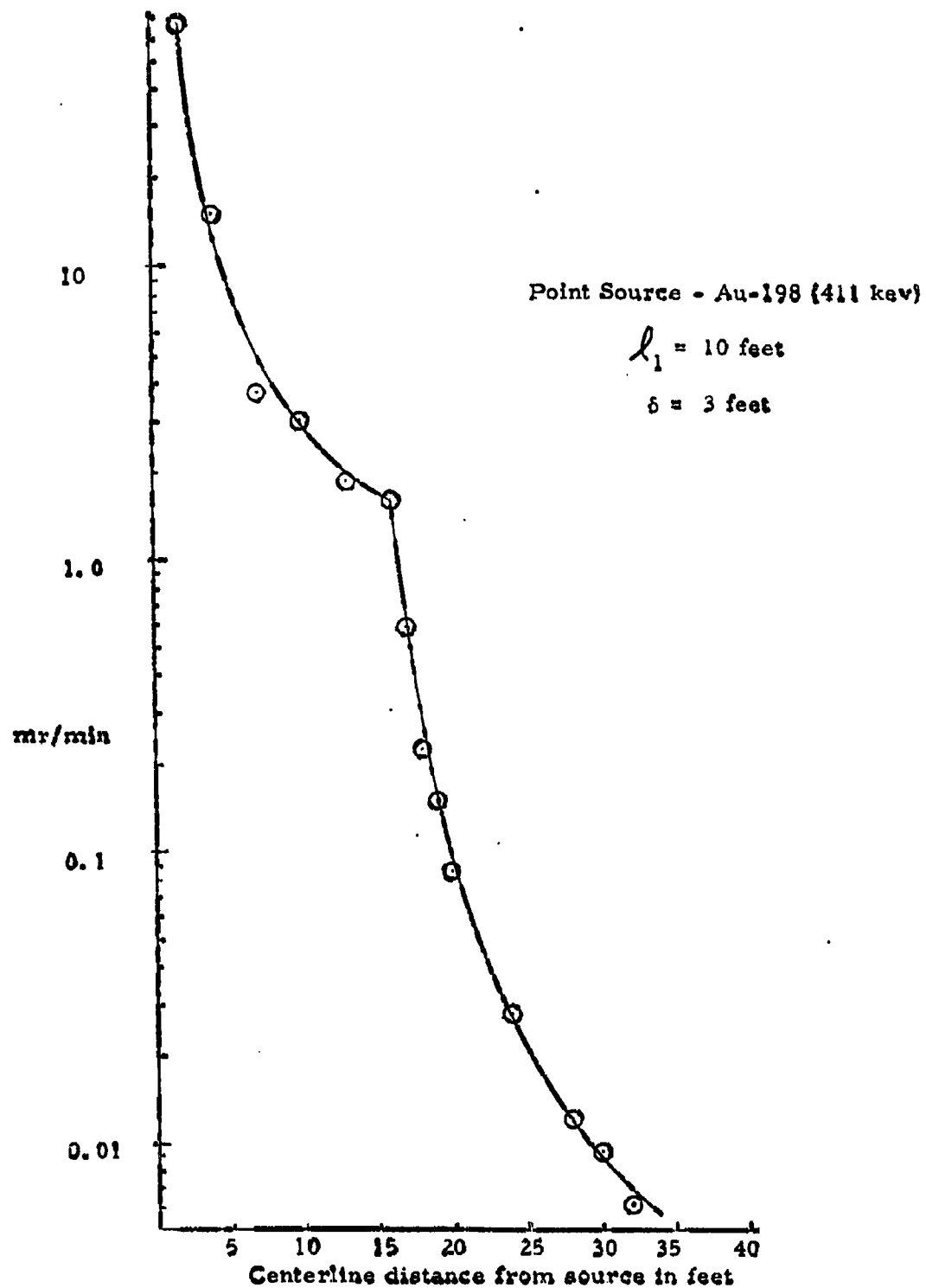


Figure 16. Measured Gamma Dose Rate Centerline Distribution in 6 by 6 Foot Concrete Entranceway with Single Right Angle Bend  
 ARMOUR RESEARCH FOUNDATION OF ILLINOIS INSTITUTE OF TECHNOLOGY

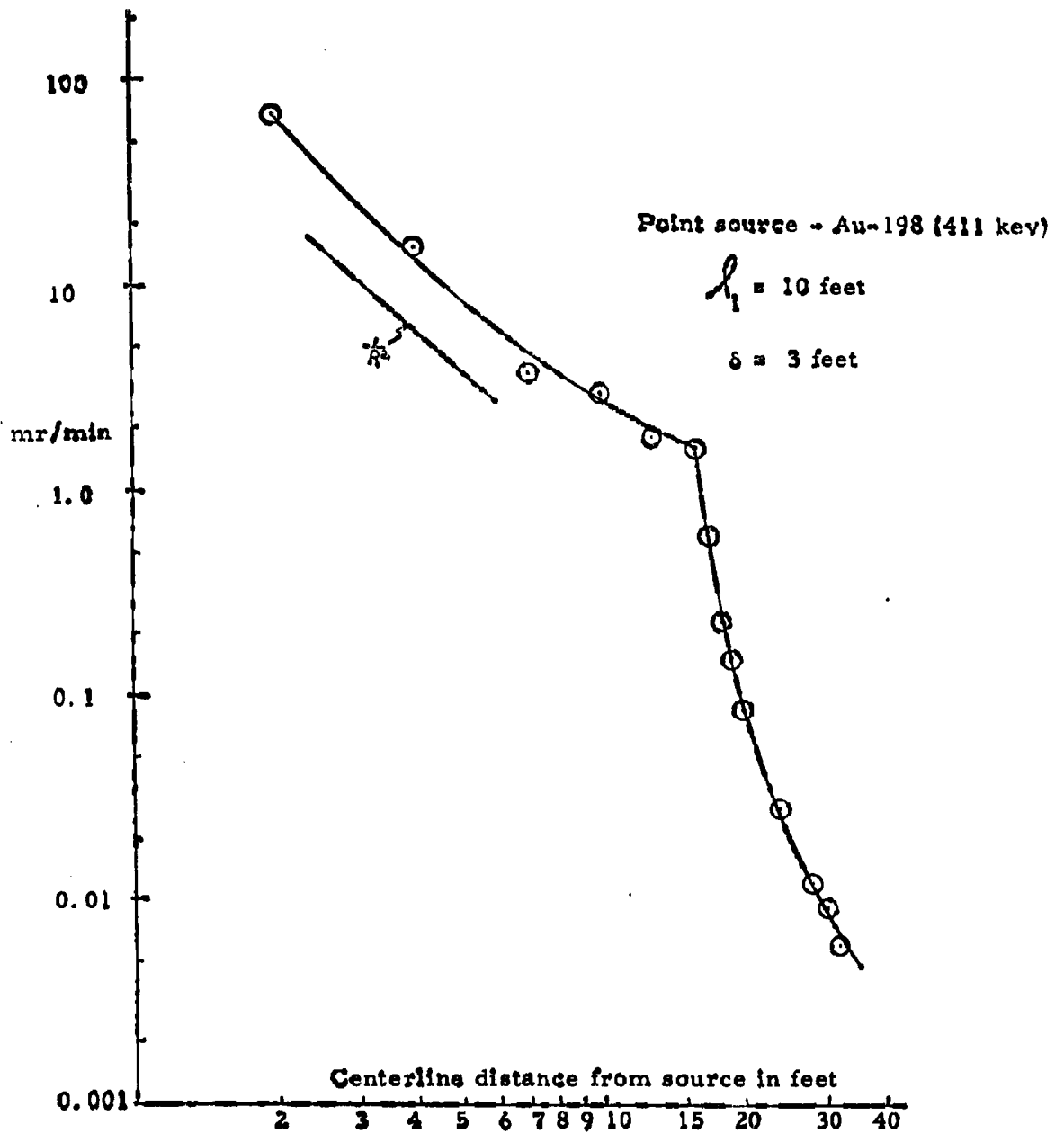


Figure 17. Measured Gamma Dose Rate Centerline Distribution in 6 by 6 Foot Concrete Entranceway with Single Right Angle Bend

TABLE VI

Gamma Dose Rate Measurement in 6 by 6 Foot Concrete Entranceway  
Au-198 Point Source at S<sub>7</sub>

Measurement position	Centerline distance from source (ft)	$h_1$ (ft)	$h_2$ (ft)	Dose rate (mr/min)	Dose attenuation factor
1	29	7	16	0.0123	249
1a	27	7	14	0.0168	182
2	25	7	12	0.0229	134
3	21	7	8	0.0537	57.1
4	17	7	4	0.175	17.5
4a	16	7	3	0.251	12.2
4b	15	7	2	0.376	8.15
4c	14	7	1	2.44	1.26
5	13	7	--	2.61	1.18
6	10	7	--	3.07	-----
7	7	7	--	5.73	-----
8	4	7	--	16.4	-----
8a	2	7	--	67.2	-----

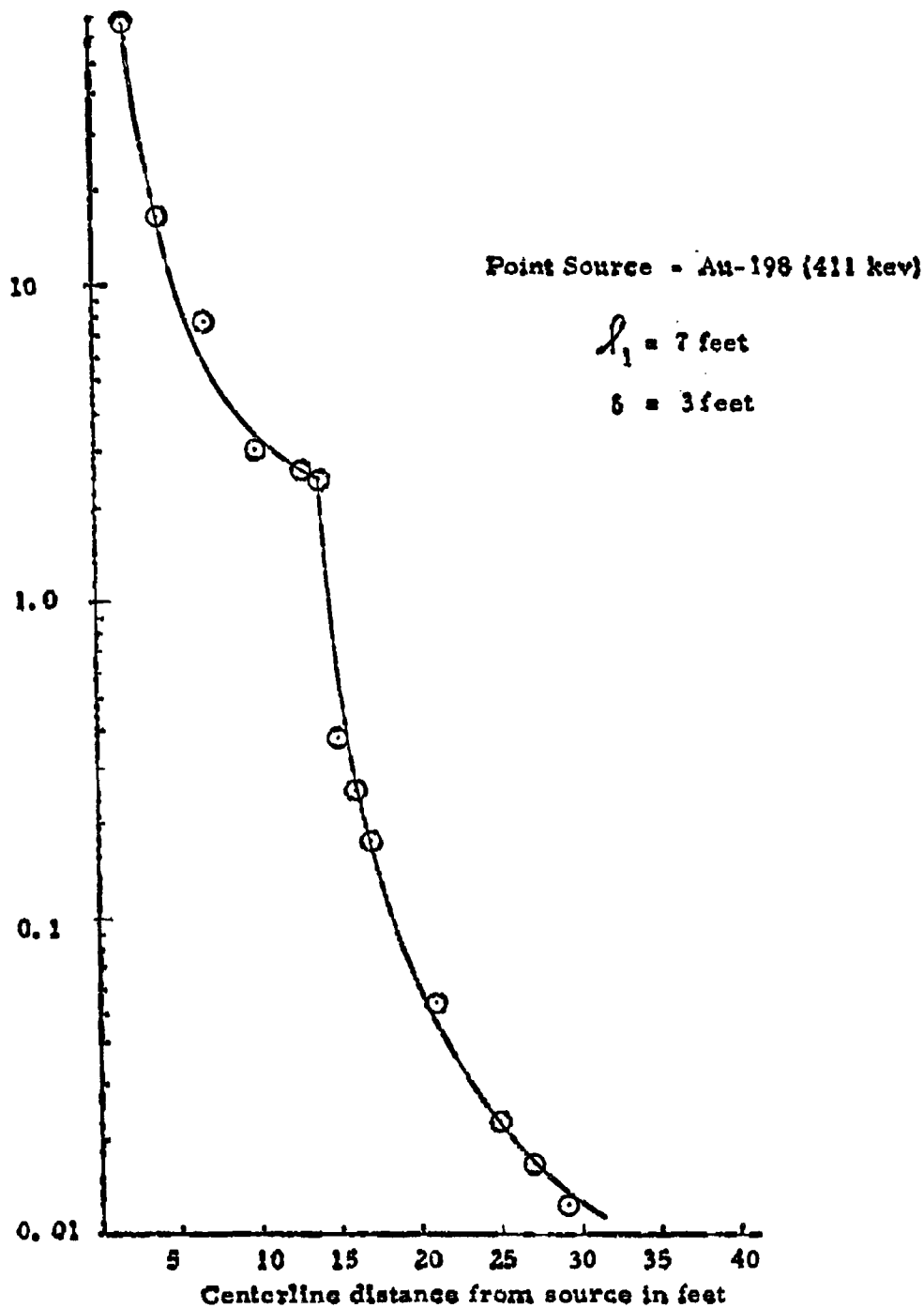


Figure 18. Measured Gamma Dose Rate Centerline Distribution  
in 6 by 6 Foot Concrete Entranceway with Single Right Angle Bend  
ARMOUR RESEARCH FOUNDATION OF ILLINOIS INSTITUTE OF TECHNOLOGY

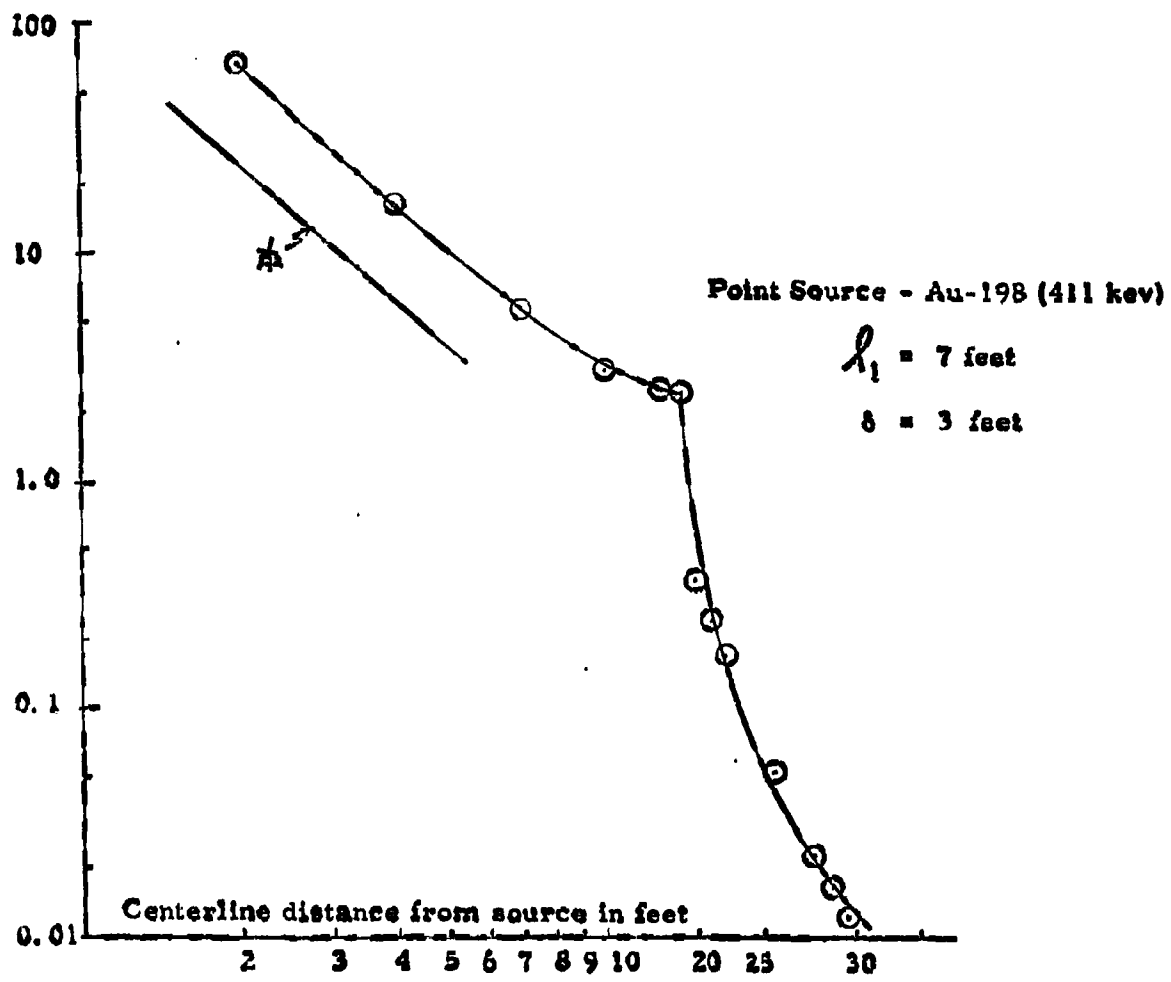


Figure 19. Measured Gamma Dose Rate Centerline Distribution in 6 by 6 Foot Concrete Entranceway with Single Right Angle Bend.

1. The attenuation ratio of a duct decreases as  $l_1$  becomes shorter.
2. The attenuation ratio of a duct is larger for higher energies.
3. The performance of the second leg distribution is less sensitive to the length of  $l_1$  for low energies.

TABLE VII

Dose Attenuation Ratios Versus Energy and Length of  $l_1$

Energy	Duct half width (ft) $\delta$	$l_1$ (ft)	$l_2$ (ft)	Dose attenuation ratio
Na-24	3	7	16	588
Au-198	3	7	16	249
Na-24	3	10	16	587
Au-198	3	10	16	303
Na-24	3	14	16	715
Au-198	3	14	16	301

In Figures 20 and 21 a comparison of Na-24, Co-60 and Au-198 in the first ( $l_1$ ) and second ( $l_2$ ) legs is shown. These data are for  $l_1 = 7$  and  $\delta = 3$  feet. The Co-60 data was taken from Table V on page 55 of the previous final report, ARF-1158-12. The Na-24 and Au-198 data was normalized to the Co-60 data at position number six (6) which is

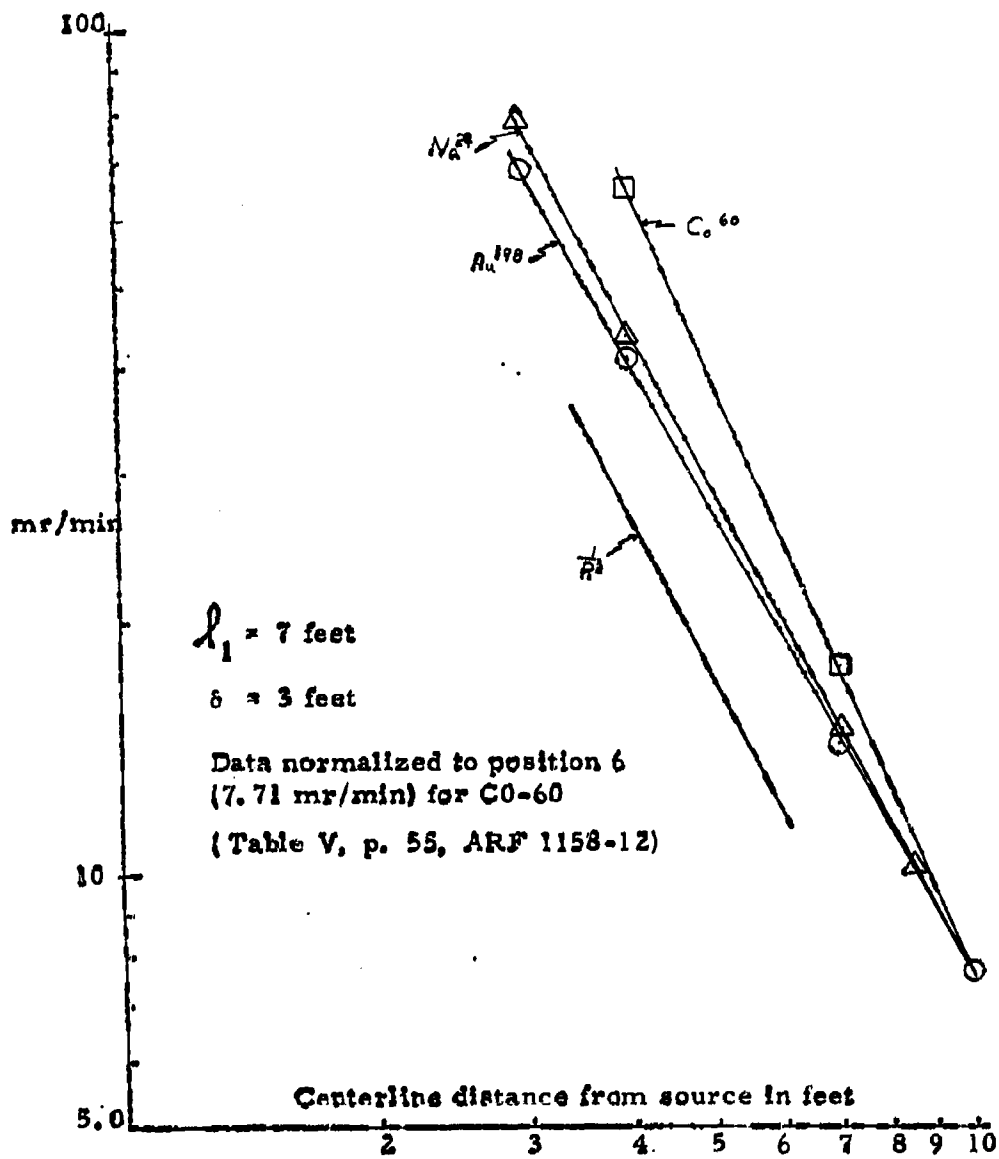


Figure 20. Comparison of First Leg ( $l_1$ ) Centerline Gamma Dose Rate Distributions for Au, Co, and Na

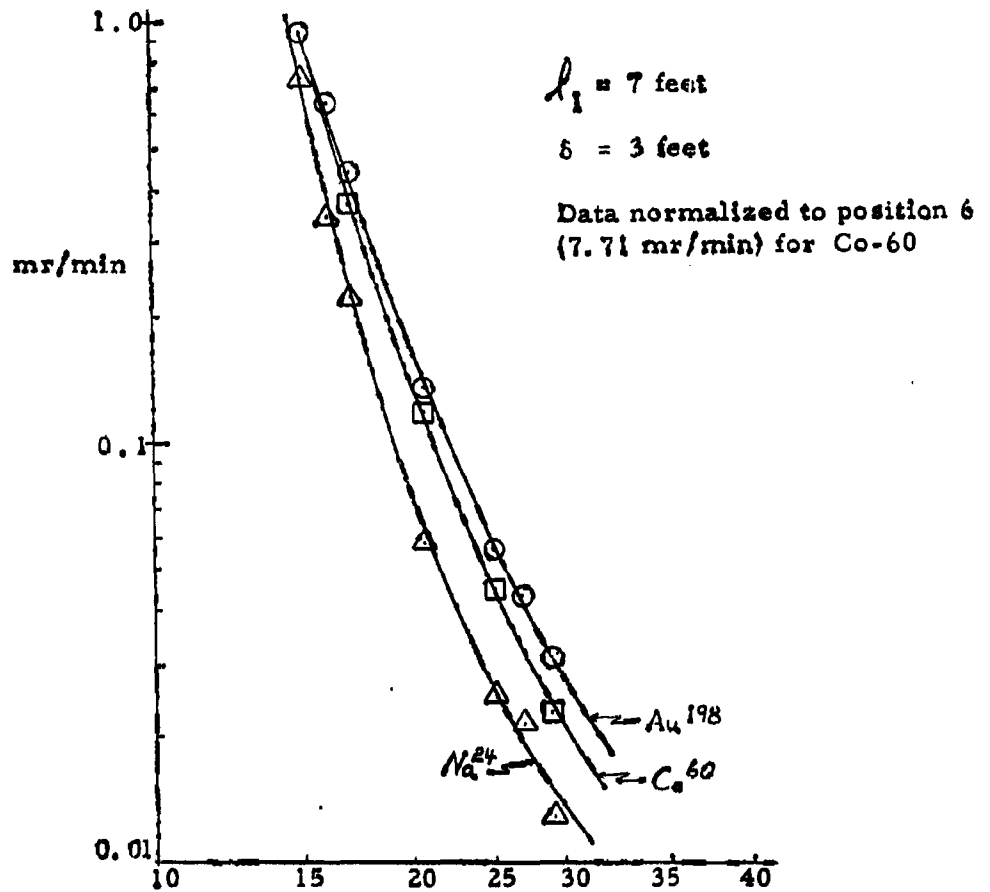


Figure 21. Comparison of Second Leg ( $l_2$ ) Centerline Gamma Dose Rate Distributions for Au, Co, and Na

is the center of the right angle bend.

A  $1/R^2$  line is drawn in Figure 20 for comparison. There is no obvious reason why the Co-60 data show a greater deviation from  $1/R^2$ . We therefore suspect the data, which was taken under slightly different conditions than the Na and Au data.

In Figure 21, for  $l_2$ , the second leg, the identical slopes are puzzling. This might be explainable on the basis that the contributions from albedo scattering from the walls of the second leg is negligible compared to the direct contribution from the four scattering surfaces which make up the right angle bend and which see both source and detector.

A tabulation of all existing ARF gamma ray data for full scale concrete personnel shelter entranceways is given in Table VIII. The attenuation factor is seen to decrease rapidly with a decrease in  $l_1$  and to also decrease rapidly as the energy decreases. Note the behavior of the attenuation ratio of Na and Au as  $l_1$  varies. This is not understood.

C. Relative Worth of the Four Scattering Surfaces which Form the Right Angle Bend

Given a duct with a fixed cross sectional area, a fixed  $l_1$  and  $l_2$ , and hence a definite attenuation ratio for gamma rays of energy E, we wish to investigate possible artificial ways of increasing that attenuation. As lead has a lower albedo than concrete, an obvious device would be to cover one or more of the surfaces at the right angle bend. Questions of importance are, what thickness of lead and which surfaces?

TABLE VIII  
Gamma Dose Attenuation Factors for Concrete Shelter Entranceways

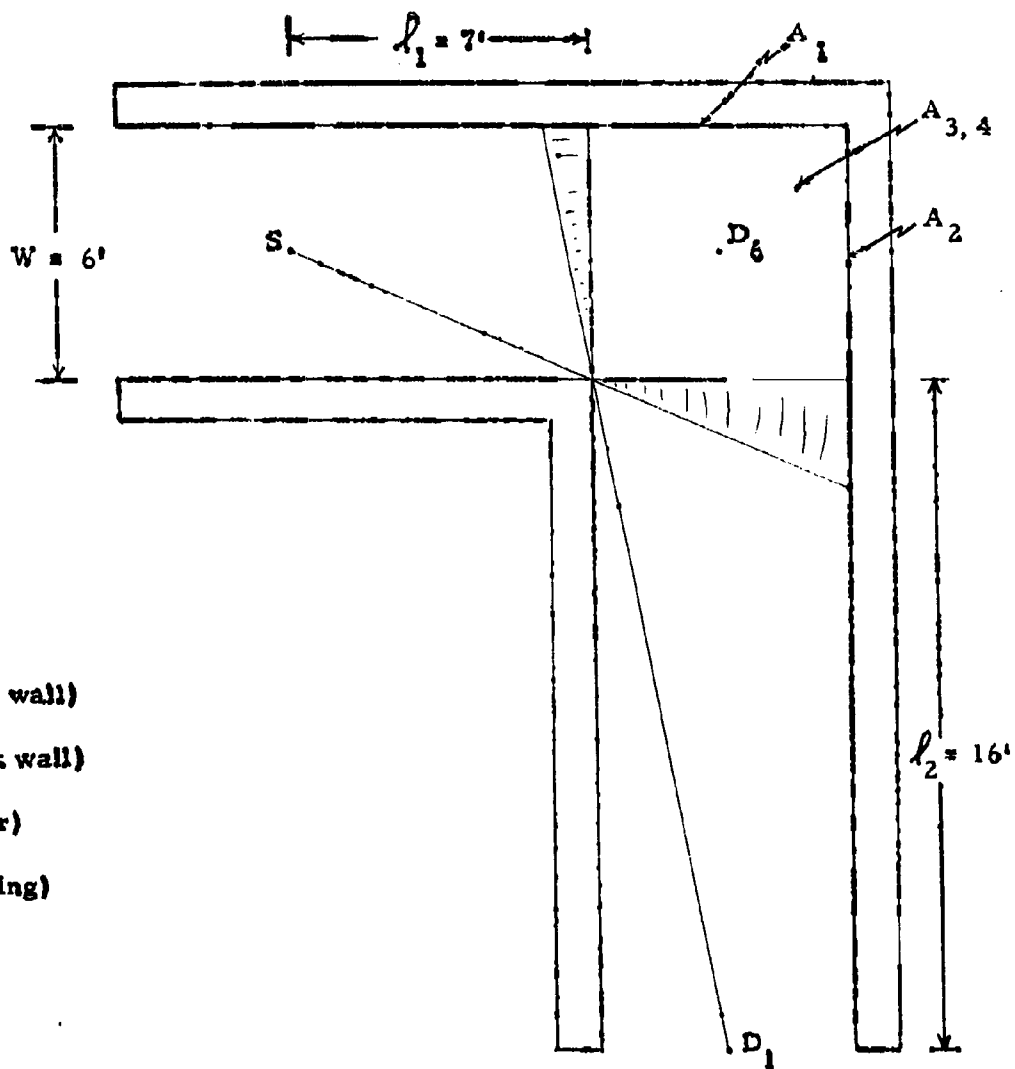
Energy	$L_1$ (ft)	$L_2$ (ft)	$\delta$ (ft)	Dose Rate (mr/min)		Dose Attenuation Ratio	Reference
				No. 6	No. 1		
Na-24 2.76 mev 1.36 mev	14	16	3	5.51	0.0077	715	Table I
Na-24 2.76 mev 1.36 mev	10	16	3	8.95	0.0152	587	Table II
Na-24 2.76 mev 1.36 mev	7	16	3	14.70	0.250	588	Table III
Co-60 1.33 mev 1.17 mev	9	16	3	6.62	0.0156	424	Table V (ARF 1158-12)
Co-60 1.33 mev 1.17 mev	7	16	3	7.71	0.0231	334	Table V (ARF 1158-12)
Co-60 1.33 mev 1.17 mev	5	16	3	12.19	0.0403	302	Table V (ARF 1158-12)
Cs-137 (0.68 mev)	9	16	3	0.818	0.00307	266	Table IV (ARF 1158-12)
Au-198 (0.411 mev)	14	16	3	0.94	0.00313	301	Table IV
Au-198 (0.411 mev)	10	16	3	1.87	0.00616	303	Table V
Au-198 (0.411 mev)	7	16	3	3.07	0.0123	249	Table VI

A four (4) curie Co-60 source was positioned in the 6 by 6 foot entranceway as shown in Figure 22 with measurements to be made at positions  $D_6$  and  $D_1$ . A lead sheet, 6 by 6 feet, was placed on the floor surface ( $A_3$ ). The data are given in Table IX.

The results show that the addition of 1/8 inch of lead to  $A_3$  (floor) reduces the dose rate  $D_1$  by about 11%. The addition of a second 1/8 inch lead sheet, giving a total lead thickness of 1/4 inch on the floor, did not further reduce the dose at  $D_1$ . The results are reasonable and are explainable by observing the average distance through the lead the incident and scattered gammas must pass. We may also conclude that 1/8 inch added to the ceiling would result in another 11% decrease, due to symmetry. The attenuation ratios shown have little value because the lead is affecting the dose rate at  $D_6$  also. We should have used another position in  $D_1$  (closer to the source) in order to have a fixed reference (unaffected by the addition of lead).

The above procedure was repeated for area  $A_1$ . The results are given in Table X. The tremendous weight of the lead (72 x 72 x 1/8 inch sheet) precluded hanging more than 1/8 inch on  $A_1$ . Clearly, 1/8 inch of lead on  $A_1$  results in a greater attenuation than on  $A_3$  or  $A_4$ . The difference ( $\sim 2\%$ ) in the no lead values of  $D_1$  (0.0223 - Table IX, and 0.0217 - Table X) is due to reproducibility of source and detector. The data in the two tables mentioned above were taken on two different days, the setup being necessarily disassembled in-between.

ARMOUR RESEARCH FOUNDATION OF ILLINOIS INSTITUTE OF TECHNOLOGY



$A_1$  (side wall)

$A_2$  (back wall)

$A_3$  (floor)

$A_4$  (ceiling)

Figure 22. Experimental Geometry for Determining Contribution from Scattering Surfaces which Form Right Angle Bend of the 6 by 6 Foot Concrete Entranceway

TABLE IX

Effect of Lead Sheet on Scattering Surface  $A_3$ 

Position	Reading (mr/min)	BNG (mr/min)	Dose Rate (mr/min)	Attenuation Ratio $D_6/D_1$	% Change in $D_1$
<u>No Lead</u>					
$D_6$	8.85	0.00065	8.85	397	-----
$D_1$	0.0229	0.00065	0.0223		
<u>1/8 Inch Lead on Area <math>A_3</math></u>					
$D_6$	8.96	0.00065	8.96	453	11.2%
$D_1$	0.0204	0.00065	0.0198		
<u>1/4 Inch Lead on Area <math>A_3</math></u>					
$D_6$	8.80	0.00065	8.80	440	10.5%
$D_1$	0.0207	0.00065	0.0200		

TABLE X

Effect of Lead Sheet on Scattering Surface  $A_1$

Position	Reading (mr/min)	BNG (mr/min)	Dose Rate (mr/min)	Attenuation Ratio $D_6/D_1$	% Change in $D_1$
<u>No Lead</u>					
$D_6$	8.45	0.00065	8.45	390	-----
$D_1$	0.0223	0.00065	0.0217		
<u>1/8 Inch Lead on Area <math>A_1</math></u>					
$D_6$	8.31	0.00065	8.31	462	17%
$D_1$	0.0186	0.00065	0.018		

To simulate a perfect radiation trap the lead was removed and the wall represented by area  $A_4$  (ceiling) was removed completely. The dose rate at  $D_1$  decreased by 18%. Comparison with the data of pages 55 and 61 of the previous final report (ARF 1158-12) show an 18% reduction also. The reproducibility here is gratifying.

Finally, areas  $A_1$  and  $A_2$  were separately removed to determine their worth. A summary of the results is as follows:

Area	Reduction in $D_1$ dose rate due to removal of area
$A_1$	22%
$A_2$	10%
$A_3$	18%
$A_4$	18%

Referring again to Figure 22 note that, for example, area  $A_3$  is not defined so as to represent the entire area of the floor seen by the detector at  $D_1$ . The shaded areas, seen by the source and detector, will contribute to the reading at  $D_1$  along with  $A_3$ . Thus, the reductions in dose rate represent the specific total contribution that only the designated area ( $A_3$ ) makes to  $D_1$ . The sum of the four area contributions does not therefore, add to the total reading at  $D_1$ , because of the contributions due to the shaded areas and any corner effect contribution.

In attempting to draw conclusions based on the measured data, caution must be exercised. The measurements show that each of the areas

reduces the dose rate at  $D_1$  by approximately 20%, except  $A_2$ , which gives 10%. The measurements, however, say nothing about the absolute quantity (dose) of radiation from each area.

Consider  $A_2$  versus  $A_3$ . The incident angle for  $A_2$  is  $0^\circ$ . The incident angle for  $A_3$  is  $73^\circ$ . At 1 mev, the albedo for  $0^\circ$  incidence is only  $1/5$  of the albedo at  $73^\circ$ . Or consider  $A_1$  versus  $A_3$ . The angle of incidence is the same, but the angles of emergence to reach the detector directly are in two different planes. This difference cannot be evaluated as no real differential albedo emergence angle dependence is known to exist.

Finally, it must be emphasized that the reduction in the dose rate due to removal of any one of the four areas has an  $l_1$ ,  $l_2$ , and  $\delta$  dependence. As  $l_1$  and  $l_2$  increase, the shaded areas of Figure 22 will decrease and for a shorter  $l_1$  the effect of any one scattering area will diminish. Also, this experiment was done with a long  $l_2$  in order to reduce corner effect contributions to  $D_1$  to a minimum ( $\sim 1\%$ ).

D. Thermal Neutron Flux Distribution Measurement from Plane Thermal Source

During the first year of the program measurements of epithermal and sub-cadmium neutron centerline flux distributions were made. (See pages 71 and 79 of ARF 1158-12). Attenuation ratios were found to be small and the agreement between measurement and calculation was poor. The poor agreement was believed to be due to lack of any differential

neutron albedo information needed for the calculations. Also, evidence was obtained which indicated the neutron number albedo was much larger than gamma albedos and a single measurement gave a value of 0.675 for the epi-cadmium neutron number albedo.

The second year neutron effort attempted to increase the accuracy of measurements and to investigate the effect of plane sources. The sections to follow report the results of these measurements and describe the conditions of the experiments.

#### 1. Source

As the full scale 6 by 6 foot concrete walled shelter entranceway is built so that the face of the graphite thermal column of the Armour Research Reactor covers the entire entrance of leg  $L_1$ , this graphite face can be used as a source of neutrons. The geometry of the experiment is shown in Figure 23.

As we were interested in sub-cadmium neutrons (we will call them thermal), we wished to be sure that the neutrons coming from the graphite face were thermal. A series of measurements, using a cadmium covered  $BF_3$  then a bare  $BF_3$ , were made. The ratio of the bare to cadmium covered count rate will be directly proportional to thermal to fast neutron flux ratio. As we had no information as to the average energy of the fast (epi-cadmium neutrons) no energy sensitivity corrections to the fast count were made.

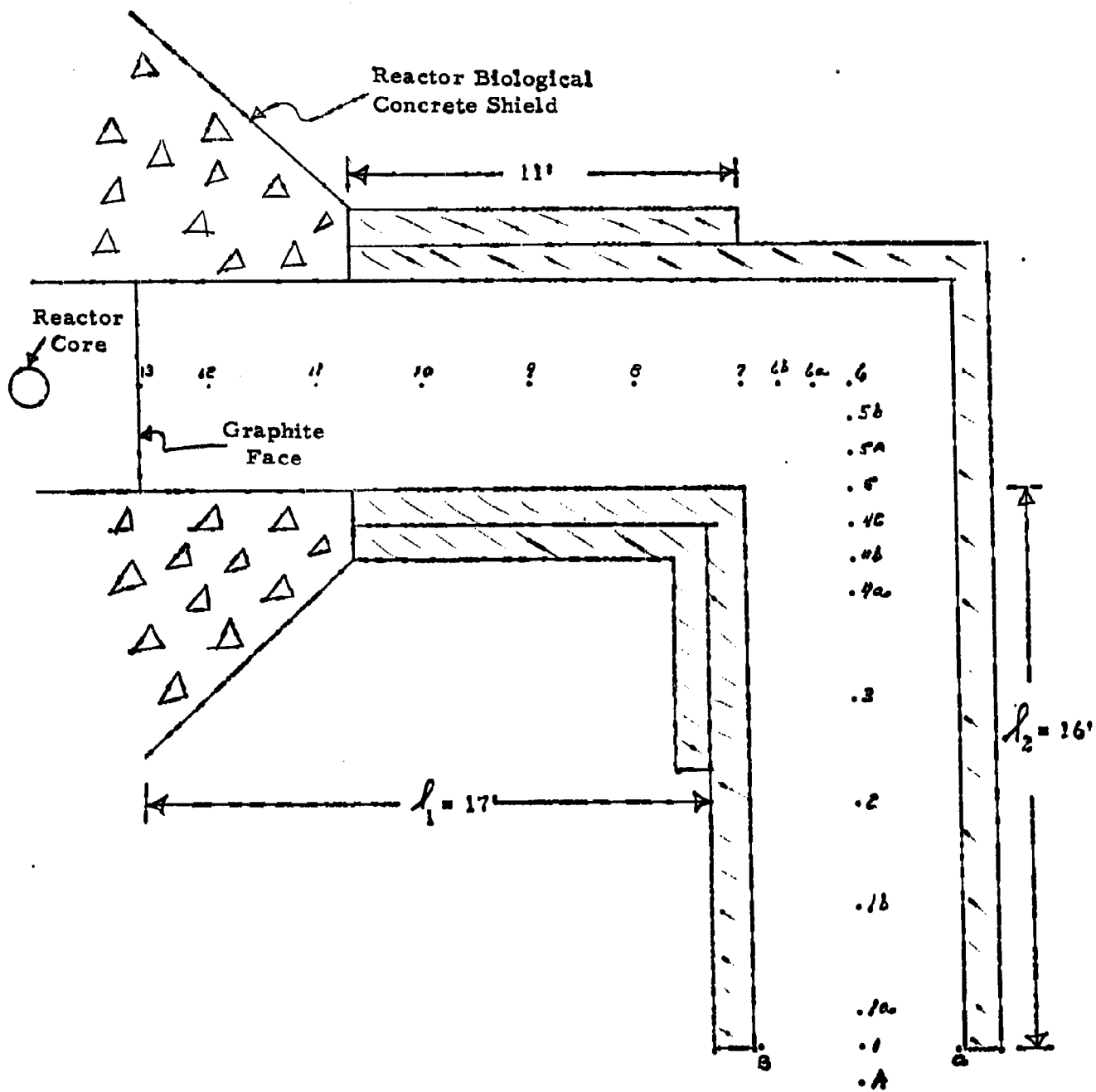


Figure 23. Thermal Neutron Distribution Measurements

ARMOUR RESEARCH FOUNDATION OF ILLINOIS INSTITUTE OF TECHNOLOGY

Measurements of the thermal to fast count rates were made at positions 12, 6, and 1 (Figure 23) and the ratios

$$\frac{\text{Bare - Cd}}{\text{Cd}} = \frac{\text{Thermal}}{\text{Fast}}$$

formed. These measurements indicated that 99.75% of the neutrons leaving the graphite thermal column face and entering the duct were sub-cadmium ( $< 1.44$  ev). Again, no counter efficiency correction to account for the  $1/v$  drop in the boron cross section was possible as the average epithermal neutron energy was unknown. The results are sufficiently conclusive so as to call the measured distribution thermal or sub-cadmium.

## 2. Detectors

As was mentioned in previous reports, no tissue equivalent neutron dose counters are commercially available, and as such, all our measurements are of number flux. For this purpose a new and more sensitive  $\text{BF}_3$  counter was purchased. It had a 4-1/2 inch active length and was 1 inch in diameter with an aluminum cathode and 60 cm of Hg pressure. This detector was checked for its gamma ray sensitivity. Its plateau was determined for neutrons in the gamma ray field expected to be present during the measurement and for the length of cable needed. The voltage used was 3025 volts with a 1 mv sensitivity setting on the discriminator. (The detector can be seen in Figure 6.)

### 3. Source Distribution

In order to obtain the source distribution a  $\text{BF}_3$  counter was covered by a 1/8 inch thick cadmium cylinder. Only the end area of the counter was left bare. The counter was positioned so that its axis was perpendicular to the graphite thermal column face. With the reactor at 0.1 watt power level, the counter was moved horizontally and vertically across the center of the graphite face in six inch steps. The results of these measurements are given in Table XI and plotted in Figure 24. A cosine distribution is plotted for comparison and the measured distribution can rather reasonably be described as an isotropic cosine source vertically and horizontally.

### 4. Thermal Neutron Distribution Measurements - Results

The reactor power was again raised to 0.1 watt and thermal neutron measurements made at the 24 positions indicated in Figure 23. All measurements, except positions B and C, were made on the centerline of the entranceway. Note the concentration of points at the bend and the measurements at positions labeled A, B, and C. The data are given in Table XII and plotted in Figures 25 and 26.

In Figure 26, the data from Figure 25 is replotted and labeled cosine source. In addition, previous data for a point thermal source (ARF 1158-12, Table XII, page 78), is plotted. The point source data was normalized to give the same flux at position six (6), 45,466 counts

**TABLE XI**  
**Thermal Neutron Source Distribution**  
**Reactor Power 0.1 Watt**

Position along the x axis	Distance from the left side (inches)	cts/min	Position along the y axis	Distance from the lower end (inches)	cts/min
1	0	5,175	12	0	5,600
2	6	15,919	13	6	18,583
3	12	28,636	14	12	31,755
4	18	40,745	15	18	41,997
5	24	50,716	16	24	53,867
6	30	58,700	6	30	58,700
7	36	53,945	17	36	54,173
8	42	45,151	18	42	42,386
9	48	32,096	19	48	34,035
10	54	19,090	20	54	18,811
11	60	3,519	21	60	5,192

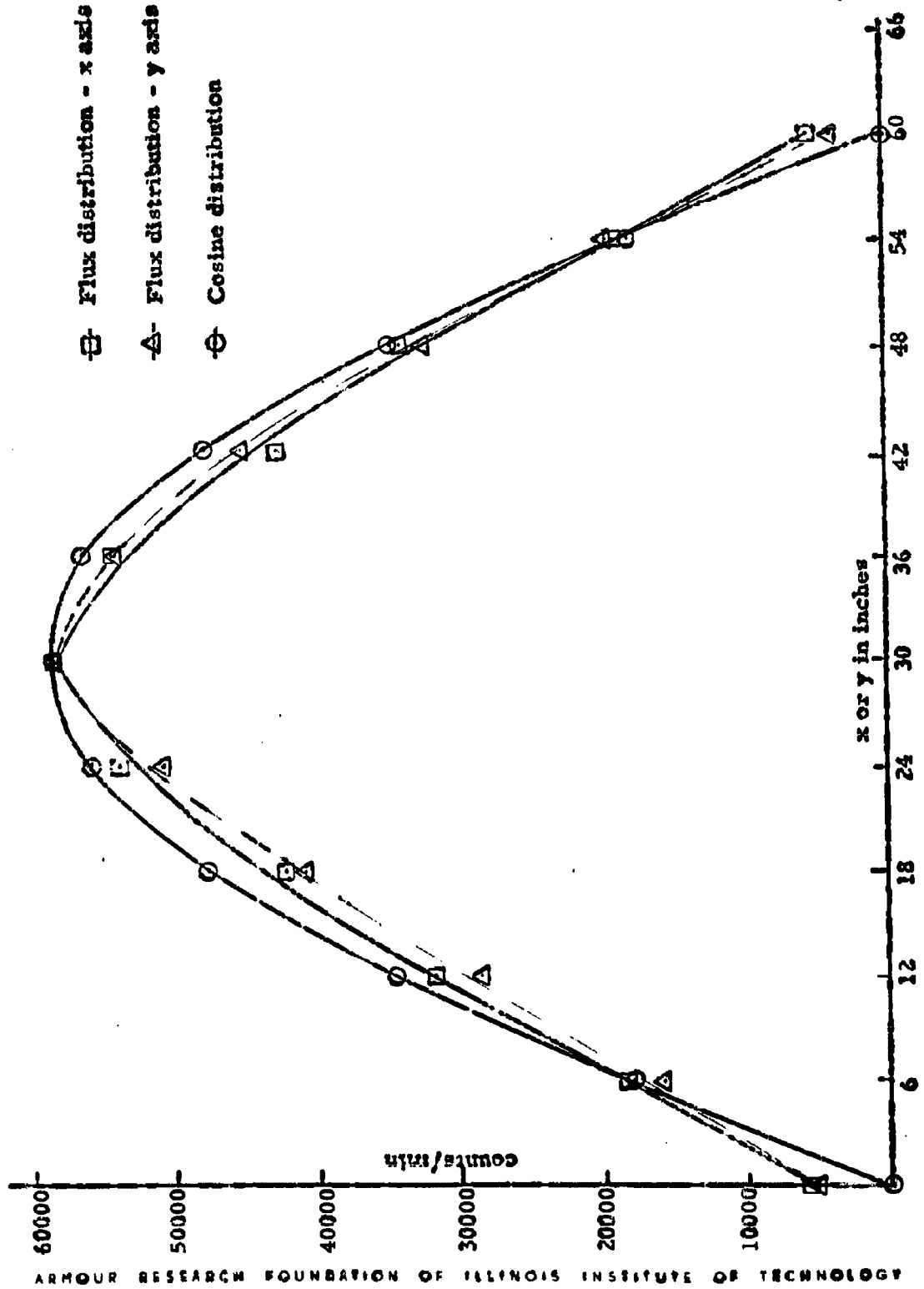


Figure 24. Thermal Neutron Distribution from Graphite Thermal Column Face.

TABLE XII

Measured Thermal Neutron Flux Centerline Distribution in 6 by 6 Foot  
Concrete Entranceway from Isotropic Cosine Thermal Neutron Source

Position	Centerline distance from source (ft)	$l_1$ (ft)	$l_2$ (ft)	$BF_3$ (counts/min)	Number attenuation ratio
A*	40	17	--	1,492	30.47
B**	--	17	--	1,602	28.38
C***	--	17	--	1,588	28.63
1	39	17	16	1,763	25.79
1a	38	17	15	2,080	20.96
1b	35	17	12	3,425	13.27
2	32	17	9	5,248	8.66
3	29	17	6	8,469	5.37
4a	26	17	3	14,340	3.17
4b	25	17	2	17,953	2.53
4c	24	17	1	21,888	2.08
5	23	17	--	35,979	1.26
5a	22	17	--	40,063	1.14
5b	21	17	--	42,847	1.06
6	20	17	--	45,466	-----
6a	19	17	--	48,152	-----
6b	18	17	--	52,350	-----
7	17	17	--	58,446	-----
8	14	17	--	80,869	-----
9	11	17	--	115,321	-----
10	8	17	--	160,275	-----
11	5	17	--	249,732	-----
12	2	17	--	672,685	-----
13	0	17	--	1,616,682	-----

\*One foot outside the second leg

\*\*three feet to the right on No. 1.

\*\*\*three feet to the left of No. 1.

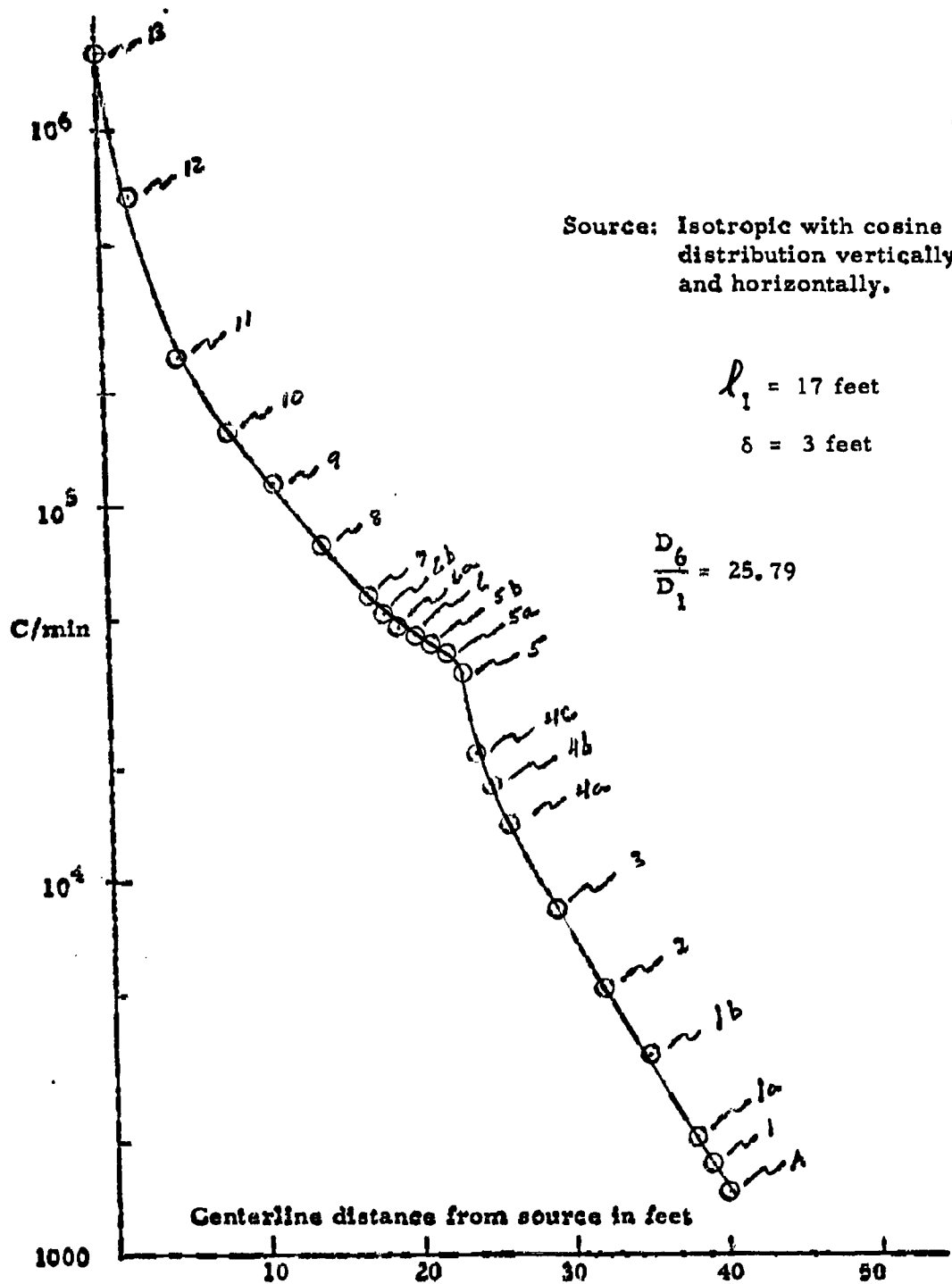


Figure 25. Measured Thermal Neutron Flux Centerline Distribution in 6 by 6 Foot Concrete Entranceway with Single Right Angle Bend

ARMOUR RESEARCH FOUNDATION OF ILLINOIS INSTITUTE OF TECHNOLOGY

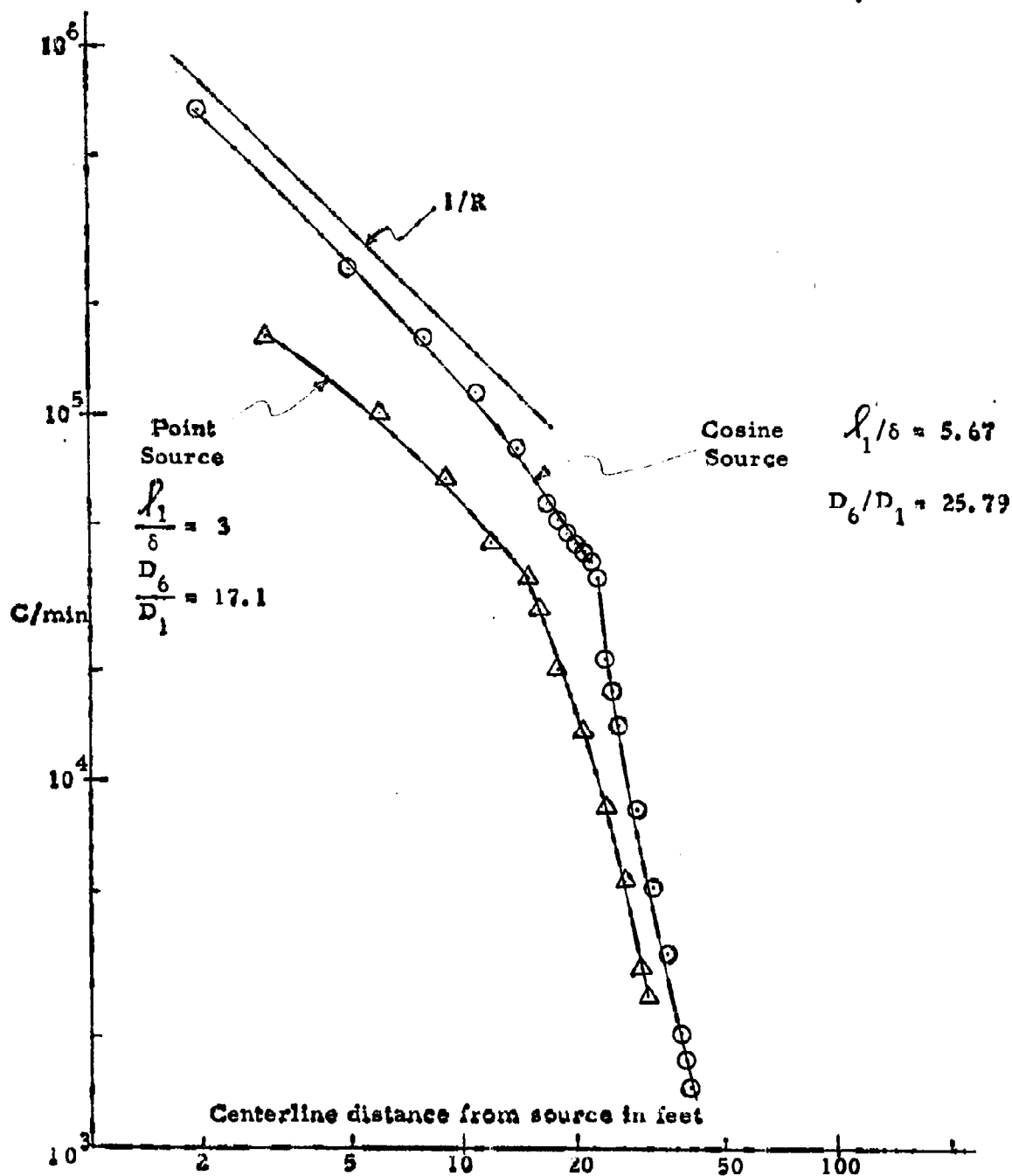


Figure 26. Comparison of Thermal Neutron Flux Centerline Distributions for Point and Cosine Isotropic Thermal Neutron Sources.

ARMOUR RESEARCH FOUNDATION OF ILLINOIS INSTITUTE OF TECHNOLOGY

per minute. Note that the  $\rho_1/\delta$  ratios are not the same and hence influence any comparison.

For convenience, a  $1/R$  line is drawn in order to observe the rate of flux fall off in the first leg for the two different sources. Recall that the gamma dose rate falls off as  $1/R^2$ .

Comparing the slopes of the cosine and point source curves with the  $1/R$  line, both fall off like  $1/R$  in the first leg ( $\mathcal{L}_1$ ). In the second leg ( $\mathcal{L}_2$ ), the cosine source curve falls faster than the point source. The attenuation ratios (No. 6/No. 1) are quite different, and disturbingly low. The cosine source has the larger attenuation ratio which is fortunate since a weapon detonated at a distance from the entrance to the shelter would appear more as a plane isotropic source, rather than a point source at the entrance.

A number of points must be borne in mind in attempting to draw conclusions from the measurements. The data is for thermal neutrons, which from a delivered dose viewpoint are grossly less important than fast neutrons. However, the shelter entrance might be located at a distance from the burst point at which a high thermal flux is present. If it is argued that the scattering surfaces at the right angle bend could be covered with boral or cadmium, the attenuation of the thermals would be large. Unfortunately, the boral or cadmium becomes a large source of hard capture gamma rays. It is not clear that we have made any gain from a delivered dose viewpoint.

ARMOUR RESEARCH FOUNDATION OF ILLINOIS INSTITUTE OF TECHNOLOGY

Second, for the point source the number distribution in  $h_1$  falls off like  $1/R$ , instead of  $1/R^2$  as the gamma distribution does, because of the magnitude of the albedo for thermal neutrons ( $\sim 0.7$ ). We believe the slower fall off in  $h_2$  for the point source may be due to the closeness of the source to the bend ( $h_1 = 9$  feet), thus increasing the corner effect contribution, ( $h_1 = 17$  feet for cosine source).

If the fast neutron dose attenuation is anywhere near as low as the number attenuation (p. 69, ARF 1158-12), a real problem exists. Greater research efforts must be placed on neutron dose distribution data and theory.

## V. SUMMARY AND CONCLUSIONS

Completion of this program has resulted in the availability of a substantial amount of measured data on radiation distributions in ducts. Such data is highly necessary input to duct and shelter design and has considerable value in that it serves as a guide to the development of analytical techniques.

Specifically, gamma ray distribution measurements were extended in energy and geometrical dependence. Thermal neutron flux distribution measurements for a non point source were made and a computer code written which has a running time of approximately two minutes and which gives dose distributions in straight square ducts.

Considerable effort was put out in order that complete details of all measurements be clear and that the calculations made and included in this report be equally clear as to methodology.

The third year of the program will concentrate on measurements in ducts of much smaller cross section than 6 by 6 feet and include a second right angle bend or third leg. The computer code will be extended to handle ducts containing right angle bends. The code will represent a significant labor saving device to project personnel and will be available for general use. Persons having a computation to be solved may prepare the program for their computer or submit the input to ARF for running here.

The Foundation is pleased to have the opportunity to conduct this program for the Bureau of Yards and Docks. We look forward to the next  
ARMOUR RESEARCH FOUNDATION OF ILLINOIS INSTITUTE OF TECHNOLOGY

phase of the program and would be equally pleased to have the opportunity to discuss other research projects.

APPENDIX I  
BIBLIOGRAPHY

ARMOUR RESEARCH FOUNDATION OF ILLINOIS INSTITUTE OF TECHNOLOGY

APPENDIX I  
BIBLIOGRAPHY

1. Barcus, J. R., TID4500 (14th Ed.) SGTM21-59(16), "Transmission of Neutrons by Cylindrical Ducts Penetrating Radiation Shields," (March, 1959).
2. Berger, M. J. and Raso, D. J., NBS Report 5982, "Backscattering of Gamma Rays," (July, 1958).
3. Clare, A. B., AERE-R2924, "The Measurement of Neutron Dose," United Kingdom Atomic Energy Authority Research Group Report, (1959).
4. Cure, J. W. and Hurst, G. S., "Fast Neutron Scattering: A Correction for Dosimetry," *Nucleonics*, Aug. 1954, pp. 36-38.
5. Davison, B., Neutron Transport Theory, Int. Series of Monographs on Physics, Oxford University Press; London (1957).
6. Eisenhauer, C. M. to LeDoux, J. C., personal communication.
7. Fisher, Edward, "The Streaming of Neutrons in Shields," *Nuc. Sci. and Engr.* 1, pp. 222-238 (1956).
8. Glass, F. M. and Hurst, G. S., "A Method of Pulse Integration Using the Binary Scaling Unit," *Rev. of Sci. Instr.* 23, No. 2, pp. 67-72, (Feb., 1952).
9. Goldstein, Herbert, Fundamental Aspects of Reactor Shielding, Addison-Wesley Pub. Co., Inc., Reading, Mass. (1959).
10. Holt, J. R. and Litherland, A. E., "A Fast Neutron Spectrometer," *Rev. of Sci. Instr.* 25, 298 (1954).
11. Hornyak, W. F., "A Fast Neutron Detector," *Rev. of Sci. Instr.*, 23, No. 6 (June, 1952).
12. Hungerford, H. E., "Some Ground Scattering Experiments Performed at the Bulk Shielding Facility," *CF-52-4-99 - Now unclassified*, (Apr. 1952).
13. Hurst, G. S., Ritchie, R. H., and Wilson, H. N., "A Count-Rate Method of Measuring Fast Neutron Tissue Dose," *Rev. of Sci. Instr.* 22, 981 (1951).

14. Hurst, G. S., and Wagner, E. B., "Special Counting Techniques in Mixed Radiation Dosimetry," Sym. on Selected Topics in Radiation Dosimetry, Vienna, Austria.
15. Johnson, D. W. and Romesberg, E. J., KAPL-2007 "Calculation of Flux to Dose Rate Conversion Factors for Fast and Intermediate Energy Neutrons."
16. Kash, S. W., "Reflection of Neutrons by a Semi-Infinite, Isotropic Scattering, Absorbing Medium." NAA-SR-275, Reactor Physics Quarterly Progress Report, May-July, 1953.
17. Kinsman, S., Ed. Radiological Health Handbook, U. S. Dept. of Health, Ed. and Welfare, Jan. 1957.
18. LeDoux, Technical Report 025, Project Y-F011-05-329, "Nuclear Radiation Shielding Provided by Buried Shelters."
19. LeDoux Technical Note N-381, Proj. Y-F011-05-329, "Analysis of the Critical Shielding Volume for Underground Shelters."
20. LeDoux, J. C., to Eisenhower, C. M., personal communication.
21. LeDoux, J. C., and Chilton, A. B., "Attenuation of Gamma Radiation Through Rectangular Ducts and Shelter Entranceways - An Analytical Approach," NCEL Technical Note N-383.
22. Patterson, H. W., Hess, W. N., Moyer, B. J., and Wallace, R. W., "The Flux and Spectrum of Cosmic-Ray Produced Neutrons as a Function of Altitude," Health Physics, Vol 2, pp. 69-72 (1958).
23. Perkins, J. F., "Monte Carlo Calculation of Gamma-Ray Albedos of Concrete and Aluminum," Jour. of App. Phys., Vol. 26, No. 6, pp. 655-658 (June 1955).
24. Peebles, G. H., R-240, "Gamma-Ray Transmission Through Finite Slabs," (Dec. 1, 1952).
25. Price, W. J., Nuclear Radiation Detection, McGraw-Hill Book Co., Inc., New York (1958).
26. Ritchie, R. H., "Calculations of Energy Loss Under the Bias in Fast Neutron Dosimetry," Health Physics 2, pp. 73-76 (1958).
27. Rockwell, T. Ed., "Reactor Shielding Design Manual," TID-7004 (1956).

28. Roe, G. M., KAPL-712, "The Penetration Neutrons Through an Empty Cylindrical Duct in a Shield."
29. Rossi, H. H., and Failla, G., "Tissue-Equivalent Ionization Chambers," *Nucleonics* 14, (2) 32 (1956).
30. Simon, A. and Clifford, C. E., CF-52-6-165 Now Unclassified, "Phenomenological Theory of the Attenuation of Neutrons by Air Ducts in Shields," (June 1952).
31. Simon, A. and Clifford, C. E., "The Attenuation of Neutrons by Air Ducts in Shields," *Nu. Sci. and Engr.* 1, 156-166 (1956).
32. Shore, F. J. and Schamberger, R. D., BNL 390 (T-74), "The Transmission of Neutrons Through Ducts in Water," (March 1, 1956).
33. Spencer, L. V., and Hubbell, J. H., NBS-Report 5659, "Report on Current Knowledge of Shielding from Nuclear Explosions."
34. Stephenson, R., Introduction to Nuclear Engineering, McGraw-Hill Book Co., Inc. New York (1958).
35. Strickler, T. D., Gilbert, H. E., and Auxier, J. A., "Fast Neutron Scattering from Thick Slabs," *Nu. Sci. and Engr.* 3, 11-18 (1957).
36. Tarks, L., KAPL-201, "Leakage of Neutrons Past a Step in an Annulus."
37. Terrall, C. W., Jerri, A., Lyday, R. O., and Sperber, D., ARF 1158-12, "Radiation Streaming in Shelter Entranceways," (June, 1960).
38. Terrall, C. W., "Radiation Streaming in Shelter Entranceways," NRDL-OCDM - Shielding Symposium Proceedings, 30 Oct. 1960, (San Francisco, Calif.).
39. Thompson, B. W., UCRL-2748, "Portable Fast and Slow-Neutron Survey Meter" (1954).
40. Vortman, L. F. (Director), WT-1218 (Feb-May, 1955), "Operation Teapot-Evaluation of Various Types of Personnel Shelters Exposed to an Atomic Explosion."
41. Wagner, E. B., and Hurst, G. S., "Advances in the Standard Proportional Counter Method of Fast Neutron Dosimetry," *Rev. of Sci. Inst.* 29, No. 2, pp. 153-158 (Feb. 1958).

42. Wagner, E. B. and Hurst, G. S., "Gamma Response and Energy Loss in the Absolute Fast Neutron Dosimeter," Health Physics 2, pp. 57-61 (1959).
43. Wilf, H. to Terrell, C. W., personal communication.
44. Whitcombe, D. W., AFCD-3413, "A Diffusion Solution for the Cylindrical Ducting Problem of Infinite Geometry."
45. Young, D. S., LA-1938, "Paraffin Cylinders to Measure Neutron Energies."
46. Chilton, A. B., "Further Analysis of Gamma Ray Attenuation in Two-Legged Rectangular Ducts, Technical Note N-383, Project Y-F011-05-329.

APPENDIX II  
FUTURE RESEARCH RECOMMENDATIONS

ARMOUR RESEARCH FOUNDATION OF ILLINOIS INSTITUTE OF TECHNOLOGY

APPENDIX II  
FUTURE RESEARCH RECOMMENDATIONS

The itemized list of suggested research problems is brief but will be clear to those knowledgeable in the field. The list is not in any order of importance, nor is it complete. We are prepared to undertake these studies and would welcome the opportunity to have suggestions as to their conduct.

1. Measurement of dose rate distribution in two leg ducts for fast neutrons from point sources to develop the theory in order to handle analytically.
2. Measurement of fast neutron dose rate distributions in 2 leg ducts for plane sources.
3. Measurement of thermal neutron flux distributions in 2 leg ducts for plane sources.
4. Measurement of fast neutron dose rate distributions in 3 leg duct (two right angle bends).
5. Experimental determination of differential (energy and angular dependence) neutron albedos.
6. Measurement of gamma dose rate at position one (1), resulting from removal of neutrons by absorbers at the right angle bend surfaces.
7. Measurement of gamma dose rate distributions in 2 leg ducts for plane isotropic sources. (Use one or two sources and employ superposition.)

8. Measurement of gamma dose rate distributions in three (3) leg ducts.
9. Measurement of differential gamma albedos.
10. Completion of the computer code to calculate the dose rate distribution and the attenuation of a duct of any geometry, any energy of source, and for any number of bends.
11. Measurement of gamma dose rate distributions specifically for fission product gammas as a function of time. A U-235 fission plate would be used as a source.
12. Measurement of neutron and gamma dose rate distributions in one by one foot cross section ducts.

APPENDIX III  
SEMI-RIGOROUS ALBEDO ANALYSIS

ARMOUR RESEARCH FOUNDATION OF ILLINOIS INSTITUTE OF TECHNOLOGY

## APPENDIX III

### SEMI-RIGOROUS ALBEDO ANALYSIS

Consider a straight rectangular duct of half thickness  $\delta$ , length  $L$  and having a wall thickness equivalent to many mean free paths for scattering of the source radiation. Let the source be a point and located on the duct centerline and in the plane of the entrance. The detector is placed on the centerline and in the exit plane of the duct.

The geometry of the problem is shown in Figure III-1. The differential wall surface area  $dA$  is on one of the four walls of the rectangular duct. The reference coordinate system is at the source.  $dA$  is a distance  $R_1$  from the source and  $R_2$  from the detector. Only the uncollided and once reflected radiation is to be considered. This is an excellent approximation for gamma rays but poor for neutrons. The uncollided flux reaching the detector is

$$\phi_u = \frac{S}{4\pi L^2} \quad (1)$$

The flux striking  $dA$  from the source is at an incident angle of  $\phi$  measured from the perpendicular to  $dA$  and is seen to be

$$\frac{S}{4\pi R_1^2} \cos \phi \quad (2)$$

The reflected or re-emission flux from  $dA$  is a fraction  $\alpha$  of that which fell on  $dA$ .  $\alpha$  is called the albedo and is a function of the type and



energy and angle of incidence of the radiation. Thus, the quantity of radiation leaving  $dA$  and reaching the detector  $D$  is

$$\frac{S}{4\pi R_1^2} \cos \theta \frac{\alpha(\theta, E)}{2\pi R_2^2} \quad (3)$$

where the re-emission distribution is taken as isotropic. Since we assume a monoenergetic source of radiation the albedo is taken as  $\alpha(\theta)$  only.

From Figure III-1, the following may be ascertained:

$$dA = dx dy$$

$$\cos \theta = \delta / R_1$$

$$R_1^2 = \delta^2 + x^2 + y^2$$

$$R_2^2 = \delta^2 + x^2 + (l - y)^2$$

The total reflected flux reaching  $D$  from the one wall surface is

$$\phi_S = 2 \int_{x=0}^{\delta} \int_{y=0}^l \frac{S}{4\pi R_1^2} \times \frac{\delta}{R_1} \times \frac{\alpha(\theta)}{2\pi R_2^2} dA \quad (4)$$

Considering that there are four symmetrical walls and substituting in the relationships from Figure III-1,

$$\phi_S = \frac{6S}{\pi^2} \int_0^{\delta} \int_0^l \frac{\alpha(\theta) dx dy}{\left[ \delta^2 + x^2 + y^2 \right]^{3/2} \left[ (l - y)^2 + x^2 + \delta^2 \right]} \quad (5)$$

The double integral is not conveniently handled analytically without the introduction of undesirable approximations (such as  $\delta/l \ll 1$ ) and in addition we wish to investigate the behavior of the integrand. Such investigation requires resorting to double numerical integration, a somewhat tedious process if any accuracy is desired.

In order to study the behavior of the integrand, the following parameters were chosen as representative of a practical duct such as a shelter entranceway.

$$l = 14 \text{ feet}$$

$$\delta = 3 \text{ feet}$$

$$\Delta x = 1 \text{ foot}$$

$$\Delta y = 1 \text{ foot}$$

$$E = 0.411 \text{ mev (Au-198)}$$

$$S = kS_0 = \frac{1 \text{ mr/hr}^* \times 1 \text{ curie}}{1.2 \times 10^3 \text{ } \gamma/\text{cm}^2\text{-sec}}$$

Berger and Raso\*\* computed the energy and incident angle dependence of gamma ray albedos in concrete. Their data for 0.2 and 0.5 mev is plotted and a linear ordinate extrapolation done to estimate 0.4 mev albedos. The data is shown in Figure III-2, plotted as a function of the cosine of the incident angle, with energy as a parameter.

\*Radiological Health Handbook [p. 139].

\*\*NBS Report 5982.

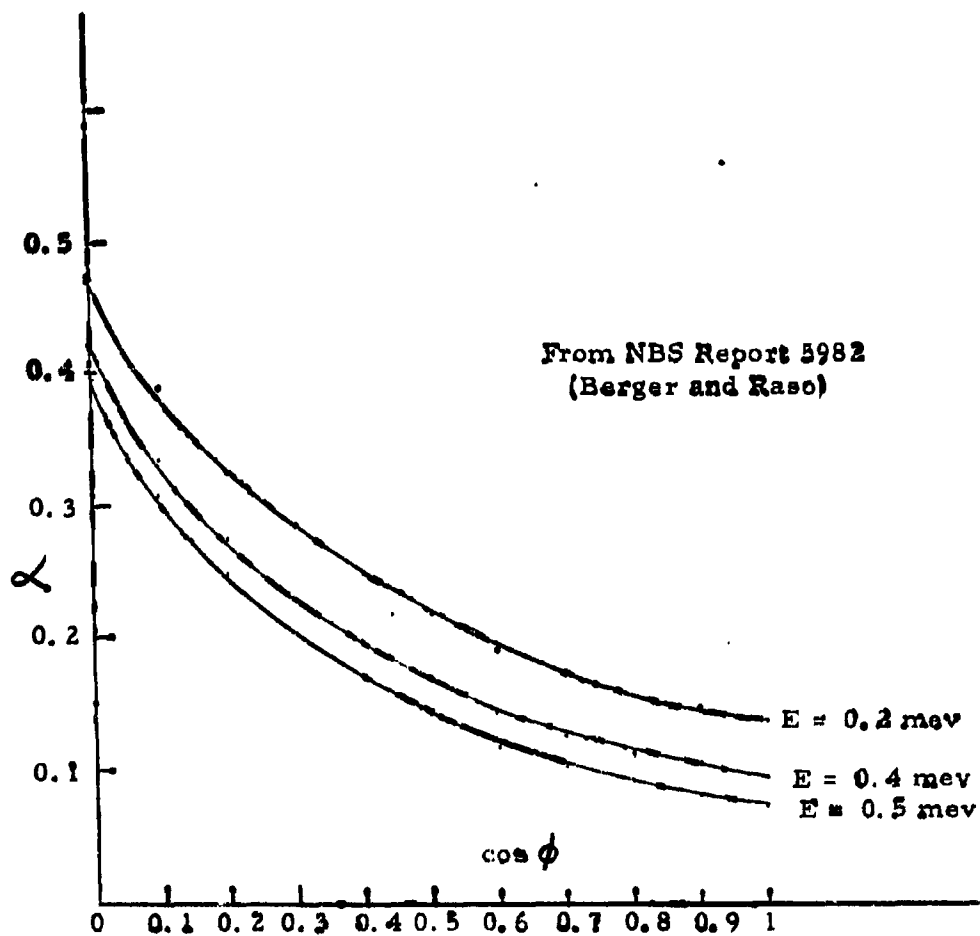


Figure III-2. Dose Albedos for Concrete as a Function of the Incident Angle.

ARMOUR RESEARCH FOUNDATION OF ILLINOIS INSTITUTE OF TECHNOLOGY

The integrand is evaluated for 15 values of  $y$  and 4 different values of  $x$  as shown in the Tables. The behavior of the integrand is seen in Figures III-3 and III-4. (The  $10^6$  factor is for convenience.) Recall that the source is at  $y = 0$  and the detector at  $y = l = 14$  feet. We see that the wall section closest to the duct center ( $x = 0$ ) and the general wall area nearest the source ( $y = 0$  to 3 feet) will contribute heavily to the integrated value of  $I(x, y)$ . Also, that the area near the detector ( $y = 11$  to 14 feet) is more important than the area near the center of the duct.

Numerical integration of the four areas yields

$$I(x_0) = 150.88$$

$$I(x_1) = 140.74$$

$$I(x_2) = 116.55$$

$$I(x_3) = 89.85$$

In Figure III-4,  $I(x)$  is plotted against  $x$  and a second integration again performed by the trapezoid rule resulting in  $I(x, y) = 378.63$ . We have expressed the source in equation (5) in terms of dose, hence the solution to five (5) required dose albedos and gives the answer in dose.

$$D_s = \frac{6S_0 k}{10^6 \pi^2} \iint I(x, y) dx dy = \frac{3 \times 3.7 \times 10^{10}}{10^6 \times \pi^2 \times 1.2 \times 10^3} [378.63] \times \frac{1}{(30.48)^2} \times \frac{1}{60}$$

$$= 0.0642 \text{ mr/min.}$$

TABLE I

x	y	$R_1 \left[ \frac{2z^2 + 2}{x+y+\delta} \right]^{1/2}$	(A) $\left[ \frac{2z^2 + 2}{x+y+\delta} \right]^{3/2}$	(B) $(x-y)^2 + z^2 + \delta^2$	(C) (A)x(B)	$\cos \phi$	(D) $\frac{\delta}{R_1}$	$\alpha(\phi)$	$\frac{(D)}{(C)} \times 10^6$
0	0	3	27	205	5535	1.000	0.095	0.095	17.16
0	1	3.162	31.622	178	5628.80	0.9487	0.10	0.10	17.76
0	2	3.6055	46.871	153	7171.26	0.8320	0.111	0.111	15.47
0	3	4.2426	76.365	130	9927.45	0.7071	0.126	0.126	12.69
0	4	5	125	109	13625	0.6	0.145	0.145	10.64
0	5	5.831	198.252	90	17842.68	0.5145	0.166	0.166	9.30
0	6	6.7082	301.868	73	22036.36	0.4472	0.185	0.185	8.39
0	7	7.6158	441.719	58	25619.70	0.3939	0.200	0.200	7.81
0	8	8.544	623.711	45	28067	0.3511	0.213	0.213	7.59
0	9	9.4868	853.806	34	29029.4	0.3162	0.225	0.225	7.75
0	10	10.440	1137.89	25	28447.2	0.2873	0.238	0.238	8.37
0	11	11.4017	1482.207	18	26679.72	0.2631	0.247	0.247	9.26
0	12	12.3693	1892.498	13	24602.47	0.2425	0.257	0.257	10.45
0	13	13.3416	2374.78	10	23747.8	0.2249	0.265	0.265	11.16
0	14	14.31782	2935.14	9	26416.26	0.2095	0.273	0.273	10.33

TABLE II

x	y	$R_1 \left[ \frac{2x^2 + 2y^2}{x^2 + y^2 + 6} \right]^{1/2}$	(A) $\left[ \frac{2x^2 + 2y^2}{x^2 + y^2 + 6} \right]^{3/2}$	(B) $(x-y)^2 + x^2 + y^2$	(C) (A)x(B)	cos $\frac{\delta}{R_1}$	(D) $\alpha(\psi)$	I(y) $\frac{(D)}{(C)} \times 10^6$
1	0	3.162	31.6225	206	6514.23	0.949	0.100	15.35
1	1	3.317	36.4820	179	6530.30	0.905	0.104	15.92
1	2	3.742	52.3829	154	8066.96	0.802	0.114	14.13
1	3	4.359	82.8191	131	10849.30	0.688	0.130	11.98
1	4	5.109	130.7288	110	14380.17	0.587	0.148	10.29
1	5	5.916	207.0649	91	18842.91	0.507	0.167	8.86
1	6	6.78	311.9830	74	23086.74	0.442	0.185	8.01
1	7	7.681	453.1795	59	26737.59	0.391	0.201	7.52
1	8	8.602	636.5664	46	29282.06	0.349	0.215	7.34
1	9	9.539	868.0868	35	30383.04	0.314	0.226	7.44
1	10	10.488	1153.693	26	29996.03	0.286	0.238	7.93
1	11	11.446	1499.354	19	28487.73	0.262	0.248	8.70
1	12	12.410	1911.056	14	26754.78	0.242	0.257	9.61
1	13	13.380	2394.863	11	26343.49	0.224	0.265	10.06
1	14	14.353	2951.362	10	29513.62	0.209	0.273	9.25

TABLE III

x	y	$R_1$		(A)	(B)	(C)	cos	(D)	$I(y)$
		$\left[ \frac{2x^2 + 2y^2}{x^2 + y^2 + 6} \right]^{1/2}$	$\left[ \frac{2x^2 + 2y^2}{x^2 + y^2 + 6} \right]^{3/2}$						
2	0	3.605	46.871	209	9796.12	0.832	0.112	11.43	
2	1	3.7416	52.383	182	9533.69	0.802	0.115	12.06	
2	2	4.123	70.092	157	11004.52	0.728	0.125	11.36	
2	3	4.690	103.188	134	13827.19	0.640	0.140	10.12	
2	4	5.385	156.164	113	17646.53	0.557	0.156	8.84	
2	5	6.164	234.246	94	22019.12	0.487	0.173	7.86	
2	6	7.000	343.000	77	26411.00	0.429	0.190	7.19	
2	7	7.874	488.187	62	30267.59	0.381	0.204	6.74	
2	8	8.775	675.657	49	33107.19	0.342	0.217	6.55	
2	9	9.695	911.347	38	34631.18	0.309	0.229	6.61	
2	10	10.630	1201.191	29	34834.54	0.282	0.240	6.89	
2	11	11.576	1551.147	22	34125.23	0.259	0.250	7.32	
2	12	12.530	1976.210	17	33442.57	0.239	0.258	7.71	
2	13	13.491	2455.293	14	34374.10	0.222	0.265	7.71	
2	14	14.457	3021.458	13	39278.95	0.207	0.275	7.00	

TABLE IV

x	y	$R_1 \left[ \frac{2x^2 + 2y^2}{x^2 + y^2 + 6} \right]^{1/2}$	(A) $\left[ \frac{2x^2 + 2y^2}{x^2 + y^2 + 6} \right]^{3/2}$	(B) $(x-y)^2 + x^2 + y^2$	(C) (A)x(B)	cos $\frac{\delta}{R_1}$	(D) $\alpha(\phi)$	I(y) $\frac{(D)}{(C)} \times 10^6$
3	0	4.2426	76.365	214	16342.11	0.7071	0.127	7.77
3	1	4.3569	82.8191	187	15487.17	0.6882	0.130	8.39
3	2	4.6904	103.188	162	16716.45	0.6396	0.140	8.37
3	3	5.1961	140.292	139	19500.59	0.5773	0.152	7.79
3	4	5.8309	198.252	118	23393.73	0.5145	0.166	7.10
3	5	6.5574	281.965	99	27914.53	0.4575	0.181	6.48
3	6	7.3484	396.806	82	32538.09	0.4082	0.195	5.99
3	7	8.1853	548.408	67	36743.33	0.3665	0.208	5.66
3	8	9.0554	742.542	54	40097.27	0.3313	0.221	5.51
3	9	9.94987	985.036	43	42356.55	0.3015	0.232	5.48
3	10	10.8627	1281.78	34	43580.05	0.2762	0.243	5.58
3	11	11.7898	1638.77	27	44246.79	0.2544	0.252	5.69
3	12	12.7279	2061.91	22	45362.02	0.2357	0.260	5.73
3	13	13.6748	2557.19	19	48586.61	0.2194	0.269	5.53
3	14	14.6287	3130.52	18	56349.36	0.2051	0.275	4.88

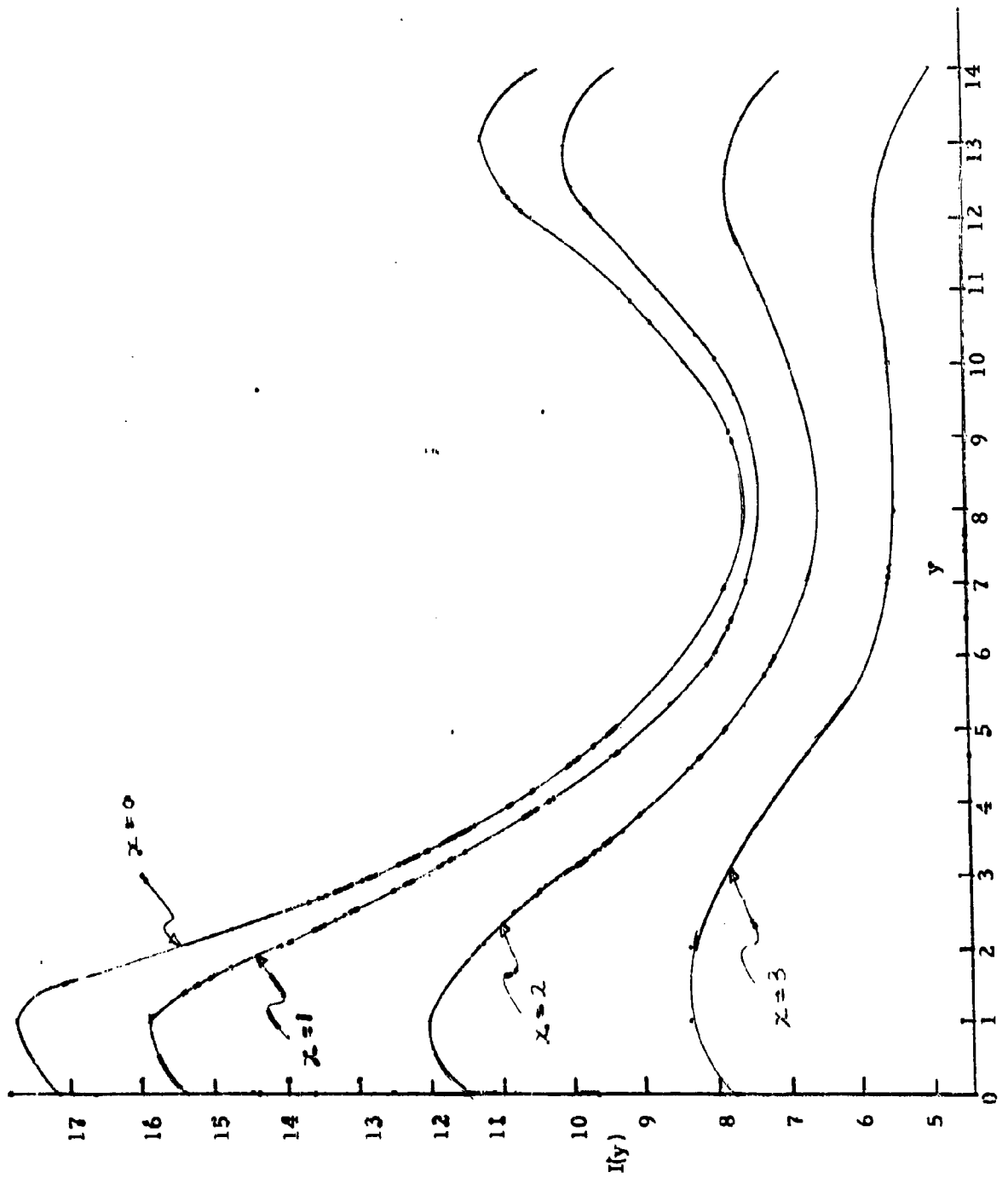


Figure III-3. Plot of Integrand  $I(x, y)$

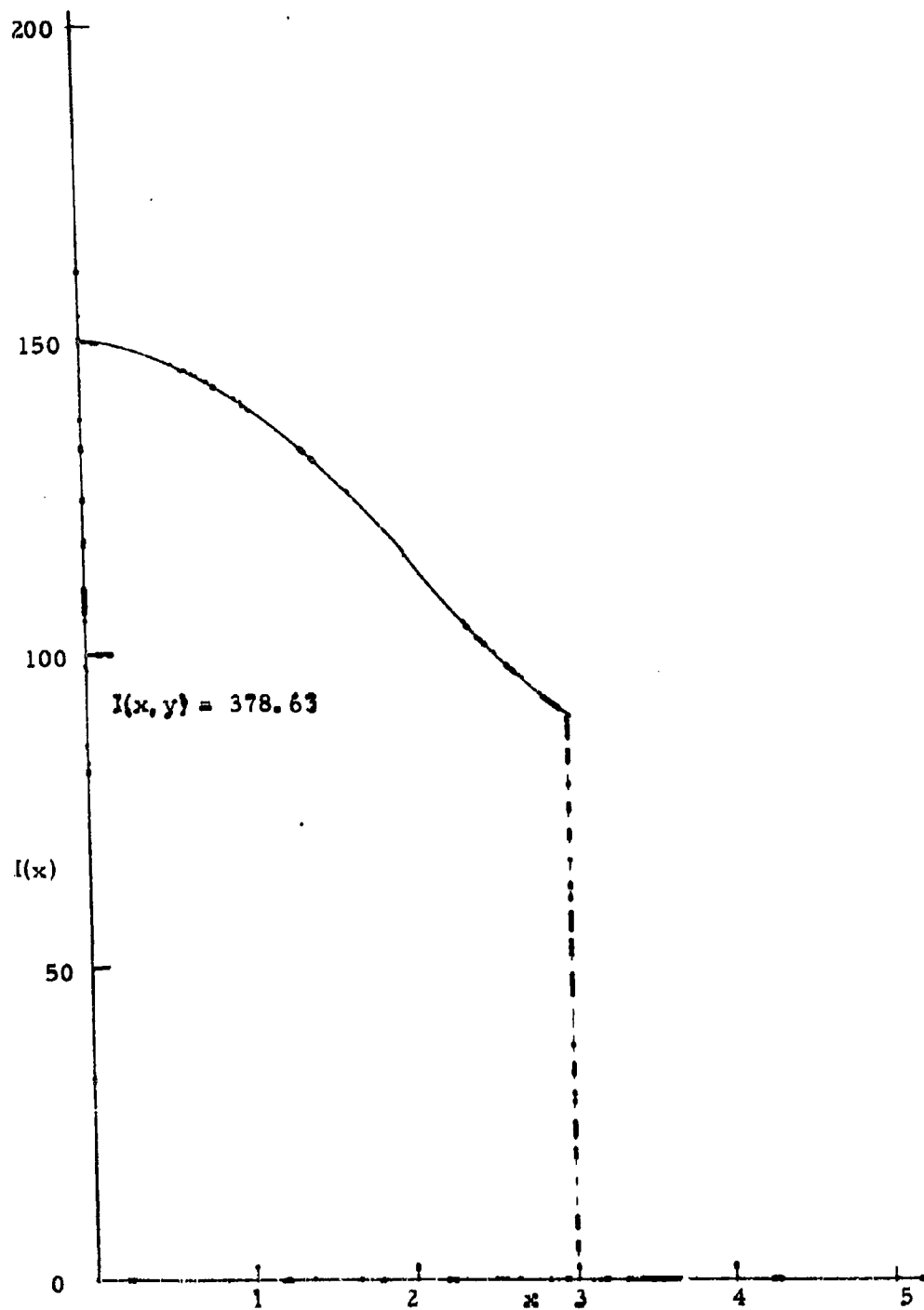


Figure III-4. Plot of Integrand  $I(x, y)$

ARMOUR RESEARCH FOUNDATION OF ILLINOIS INSTITUTE OF TECHNOLOGY

The uncollided dose is

$$D_u = \frac{Sk}{4\pi r^2} = 0.225 \text{ mr/min-Curie}$$

The total dose rate seen by the detector, 14 feet from a one(1) curie point source of Au-198 ( $E \sim 0.41$  mev) inside a 6 by 6 foot rectangular duct is

$$\begin{aligned} D_D &= D_S + D_u \\ &= 0.225 + 0.064 \\ &= 0.29 \text{ mr/min per curie.} \end{aligned}$$

The albedo scattered contribution ( $D_S$ ) to the total ( $D_D$ ) is seen to be approximately 22%.

We now wish to have an experimental check as to the validity of the analytical approach. We may obtain this by referring to Table IV. At position 7 the source is 14 feet away. The measured value is 1.62 mr/min from a source of unknown curie strength and we assume the wall behind the detector to make a negligible contribution. We have determined that 22% of the reading is due to albedo scattering. Therefore,  $1.62 \times 0.78 = 1.27$  mr/min direct from the source. For a point source of 1 curie of Au-198 we have

5 mr/min at 3 feet\* or 0.23 mr/min at 14 feet.

For the direct value of 1.27 mr/min the source strength, at the time of the measurement, must have been  $\frac{1.27}{0.23} = 5.5$  curies.

---

\* Radiological Health Handbook (p. 139).

Using the 5.5 curie gold source, we measure a dose rate of 1.62 mr/min at 14 feet from the source. Our analysis yields 0.29 mr/min-  
Curies x 5.5 curies = 1.60 mr/min, some 1% low.

The computer program described in Section III and in Appendix IV, was given the problem with a six (6) curie source.

The input statement appears as

```
=11  
10  
=14  
40  
=Y201  
0.  
.7854  
0.  
14.  
20.6  
14.  
3.  
0.  
14.  
.425  
2.1  
.05  
=c499  
2.  
=ENDATA  
=NOMORE
```

and the output as

```
10658466 00 0 14000000 02 24037515-01  
14000000 02 30000000 01 0 14000000 02  
42500000 00 21000000 01 50000000-01 20600000 02  
0
```

The total dose rate  $D_D$  at the detector = 0.10658 R/hr = 1.77 mr/min.

However, for a 5.5 curie source

$$D_D = 1.77 \times \frac{5.5}{6} = 1.62 \text{ mr/hr.}$$

Measurement - 1.62 mr/min.

Hand calculation - 1.60 mr/min.

Code calculation - 1.62 mr/min.

I

I

APPENDIX IV

IT AND FORTRAN COMPUTER PROGRAMS

ARMOUR RESEARCH FOUNDATION OF ILLINOIS INSTITUTE OF TECHNOLOGY

A UNIVAC 1105, IT PROGRAM FOR RADIATION DISTRIBUTION  
IN STRAIGHT DUCTS

1	5	Y	700	c	700	s	33	E2,4,6,	
1.	1		READ						F
2.			Y216:=(Y202-Y201)/I1						F
4.			I3:=0						F
6.			Y224:=Y207*Y207						F
7.			Y225:=Y206*Y206						F
8.			Y226:=Y208*Y208						F
9.			Y227:=Y209*Y209						F
10.			Y228:=Q6E,(Y226+Y224)Q						F
11.			Y229:=Q6E,(Y227+Y224)Q						F
12.			Y230:=Y207/Y228						F
13.			C0:=(Y210*Q2E,-Y230*Y211Q)+(Y212*Y230)						F
14.			C408:=C0						F
15.			Y0:=(Y206+Y207-(Y225+2.*Y224)/Q6E,(Y225+4.*Y224)Q						F
16.			)/(2.*Y207)						F
17.			C0:=(2.*Y207*Q6E,Y230Q)/((1-Y0*C0)*Y229)						F
18.			Y0:=Y224/(Y225+4.*Y224)						F
19.			Y0:=(Y206/(2.*Q6E,(Y225+4.*Y224)Q))*(1+Y0+(2.25*Y						F
20.			0*Y0))						F
21.			C0:=C0+(1-Q6E,Y230Q)/(1-Y0*C408)						F
22.			C0:=(C0*Y205*Y224*C408)/(Y228*Y228*Y228*Y229*Y229)						F
23.			Y231:=(Y205*.7854)/((Y209-Y208)*(Y209-Y208))						F
25.	0		TY231TY0TC0TC408						F
26.			I3:=1						F
26.5			Y221:=Y203						F
27.	33		23,15,I3,1,I4+1,						F
27.2	25		I3:=1						F
27.3	30		Y217:=Y201						F
27.4	9		a13IFY201>0.						F
27.5	28		a13IFY221>0.						F
27.6	31		Y217:=Y217+Y216						F
27.8			I3:=2						F
28.	13		3,I2,I3,1,I1+1,						F
28.6	32		I2:=I2-1						F
29.	2		C12:=Y224/(Q4E,Y217Q*Q4E,Y217Q)						F
30.			C401:=C12						F
31.			C12:=Q6E,(C12+(Y221-Y206)*(Y221-Y208))Q						F
32.			C402:=C12						F
33.			C12:=Y207/C12						F
34.			a7IFC499=0						F
35.			a8IFC499=1.						F
36.			a6IFC499=2.						F
37.	7		C403:=0						F
38.			Y230:=0						F
39.			a5						F
40.	8		C403:=1.						F
41.			Y230:=1.						F
42.			a5						F
43.	6		C403:=C12						F
44.	5		C12:=(Y210*(Q2E,(-C12*Y211)Q)+(Y212*C12)						F
45.			C404:=C12						F

46.		g191fc403=0.	F
47.		Y12:=(((Y206-Y221)*(Y206-Y221))+2.*Y224)/Q6E,	
48.		((Y206-Y221)*(Y206-Y221))+4.*Y224)Q	F
49.		Y12:=(Y206+(2.*Y207)-((Y221*Y221)+2.*Y224)/Q6E,	
50.		((Y221*Y221)+4.*Y224)Q)-Y12)/(2.*Y207)	F
51.		C12:=(2.*Y207/(1-Y12*C12))*Q6E,c403/(((Y221-Y209)*(Y	
52.		221-Y209))+C401)Q	F
53.		TY12TC12T12TC404	F
54.	19	g111fc403=1.	F
55.		Y12:=Y224/(((Y206-Y221)*(Y206-Y221))+4.*Y224)	F
56.		Y12:=1+Y12+(2.25*Y12*Y12)	F
57.		Y12:=Y12*(Y206-Y221)/Q6E,(((Y206-Y221)*(Y206	
58.		-Y221))+4.*Y224)Q	F
59.		c405:=Y12	F
60.		Y12:=Y224/((Y221*Y221)+4.*Y224)	F
61.		Y12:=(1.+Y12+(2.25*Y12*Y12))*(Y221/Q6E,((Y221*Y221)	
62.		+4.*Y224)Q)	F
62.5		TY12TC405	F
63.		Y12:=(Y12+c405)*.5	F
64.	17	g271fc403>0.	F
66.	26	C12:=0.	F
67.	27	C12:=C12+(1.-Q6E,c403q)/(1.-Y12*C404)	F
67.5		TY12TC12	F
68.	11	C12:=(C12*Y205*C404*C401)/((C402*C402*C402)*((Y221-	
69.		Y209)*(Y221-Y209))+C401))	F
70.		TY12TC12TC403TC401	F
70.5		I2:=I2+1	F
71.	3	Y217:=Y217+Y216	F
72.		Y218:=0	F
73.		4,12,2,2,11-2,	F
74.	4	Y218:=Y218+(2.*C12)+4.*C(12+1)	F
75.		Y(15+500):=(Y216/3.)*(C0+(4.*C1)+Y218+C11)	F
76.		Y220:=(Y204-Y203)/14	F
80.		C501:=Y501	F
83.	22	C(15+500):=Y(15+500)	F
84.		TC(15+500)T15	F
85.	23	Y221:=Y221+Y220	F
86.		Y222:=0	F
87.	16	24,15,3,2,14-1,	F
88.	24	Y222:=Y222+(2.*C(15+500))+4.*C(15+501)	F
88.5		TY222	F
89.		Y223:=(Y220/3.)*(C501+(4.*C502)+Y222+C(14+1))	F
90.		Y232:=Y223+Y231	F
91.	14	TY232TY203TY204TY223	F
92.	15	TY206TY207TY208TY209	F
93.		TY228TY229TY230TC408	F
94.		TY216TY220TY501TC501	F
95.	21	TY210TY211TY212TY205	F
96.	10	r(0.)	F
97.		e1	FF

Note: There is no difference between upper and lower case letters in the IT Language.

ARMOUR RESEARCH FOUNDATION OF ILLINOIS INSTITUTE OF TECHNOLOGY

AN IBM 1620, FORTRAN PROGRAM FOR RADIATION DISTRIBUTION  
IN STRAIGHT DUCTS.

```

1      DIMENSION Y(701), C(701)
      READ, I1, D1, I4, D4, C(500)
      DO 40 J=202, 213, 1
      READ, Y(J)
40     CONTINUE
      Y(217)=(Y(203)-Y(202))/D/
      I3=0
      Y(225)=Y(208)*Y(208)
      Y(226)=Y(207)*Y(207)
      Y(227)=Y(209)*Y(209)
      Y(228)=Y(210)*Y(210)
      TEMP=Y(227)+Y(225)
      Y(229)=SQR(TEMP)
      TEMP=Y(228)+Y(225)
      Y(230)=SQR(TEMP)
      Y(231)=Y(208)/Y(229)
      TEMP=(-Y(231))*Y(212)
      C(1)=(Y(211)*EXP(TEMP))+(Y(213)*Y(231))
      C(409)=C(1)
      TEMP=Y(226)+4.*Y(225)
      Y(1)=(Y(207)+Y(208)-(Y(226)+2.*Y(225))/SQR(TEMP))/(2.*Y(208))
      C(1)=(2.*Y(208)*SQR(Y(231)))/((1.-Y(1)*C(1))*Y(230))
      Y(1)=Y(225)/TEMP
      Y(1)=(Y(207)/(2.*SQR(TEMP)))*(1.+Y(1)+(2.25*Y(1)*Y(1)))
      C(1)=C(1)+(1.-SQR(Y(231)))/(1.-Y(1)*C(409))
      C(1)=(C(1)*Y(206)*Y(225)*C(409))/(Y(229)*Y(229)*Y(229)*Y(230)*Y(230))
      Y(232)=(Y(206)*.7854)/((Y(210)-Y(209))*(Y(210)-Y(209)))
      IF(SENSE SWITCH 1) 41, 42
41     PUNCH, Y(232), Y(1), C(1), C(409)
      I3=1
42     Y(222)=Y(204)
      M1=I3+1
      M2=I4+2
      DO 23 I5=M1, M2, 1
25     I3=1
      Y(218)=Y(202)
      IF(Y(202))28, 28, 13
28     IF(Y(222))31, 31, 13
31     Y(218)=Y(218)+Y(217)
      I3=2
      13     M4=I3+1
      M5=I1+2
      DO 3 M3=M4, M5, 1
32     I2=M3-1
      C(12)=Y(225)/(COS(Y(218))*COS(Y(218)))
      C(402)=C(12)
      TEMP=C(12)+(Y(222)-Y(209))*(Y(222)-Y(209))
      C(12)=SQR(TEMP)

```

```

C(403)=C(I2)
C(I2)=Y(208)/C(I2)
IF(C(500))43, 7, 43
43 IF(C(500)-1.)44, 8, 44
44 IF(C(500)-2.)7, 6, 7
7 C(404)=0.
Y(231)=0.
GO TO 5
8 C(404)=1.
Y(231)=1.
GO TO 5
6 C(404)=C(I2)
5 TEMP=(-C(I2))*Y(212)
C(I2)=(Y(211)*EXP(TEMP))+(Y(213)*C(I2))
C(405)=C(I2)
IF(C(404))45, 19, 45
45 TEMP=((Y(207)-Y(222))*(Y(207)-Y(222)))+4.*Y(225)
Y(I2)=(((Y(207)-Y(222))*(Y(207)-Y(222)))+2.*Y(225))/SQR(TEMP)
TEMP=Y(222)*Y(222)+4.*Y(225)
TEMP=((Y(222)*Y(222))+2.*Y(225))/SQR(TEMP)
Y(I2)=(Y(207)+(2.*Y(208))-TEMP-Y(I2))/(2.*Y(208))
TEMP=C(404)/(((Y(222)-Y(210))*(Y(222)-Y(210)))+C(402))
C(I2)=(2.*Y(208))/(1.-Y(I2)*C(I2))*SQR(TEMP)
IF(SENSE SWITCH 1)46, 19
46 PUNCH, Y(I2), C(I2), I2, C(405)
19 IF(C(404)-1.)47, 11, 47
47 Y(I2)=Y(225)/(((Y(207)-Y(222))*(Y(207)-Y(222)))+4.*Y(225))
Y(I2)=1.+Y(I2)+(2.25*Y(I2)*Y(I2))
TEMP=(((Y(207)-Y(222))*(Y(207)-Y(222)))+4.*Y(225))
Y(I2)=Y(I2)*(Y(207)-Y(222))/SQR(TEMP)
C(406)=Y(I2)
Y(I2)=Y(225)/((Y(222)*Y(222))+4.*Y(225))
TEMP=(Y(222)*Y(222))+4.*Y(225)
Y(I2)=(1.+Y(I2)+(2.25*Y(I2)*Y(I2)))*(Y(222)/SQR(TEMP))
IF(SENSE SWITCH 1)48, 49
48 PUNCH, Y(I2), C(406)
49 Y(I2)=(Y(I2)+C(406))*0.5
IF(C(404))26, 26, 27
26 C(I2)=0.
27 C(I2)=C(I2)+(1.-SQR(C(404)))/(1.-Y(I2)*C(405))
IF(SENSE SWITCH 1)50, 11
50 PUNCH, Y(I2), C(I2)
11 TEMP=((Y(222)-Y(210))*(Y(222)-Y(210)))+C(402)
C(I2)=(C(I2)*Y(206)*C(405)*C(402))/((C(403)*C(403)*C(403))*TEMP)
IF(SENSE SWITCH 1)51, 52
51 PUNCH, Y(I2), C(I2), C(404), C(402)
52 I2=I2+1
Y(218)=Y(218)+Y(217)
3 CONTINUE
Y(219)=0.
M6-11-1
DO 4 I2=3, M6, 2

```

```

J=I2+1
Y(219)=Y(219)+(2.*C(I2))+4.*C(J)
4 CONTINUE
J1=I5+500
J2=I1+1
Y(J1)=(Y(217)/3.)*(C(1)+(4.*C(2))+Y(219)+C(J2))
Y(221)=(Y(205)-Y(204))/D4
C(502)=Y(502)
C(J1)=Y(J1)
IF(SENSE SWITCH 1)53, 54
53 PUNCH, C(J1), I5
54 Y(222)=Y(222)+Y(221)
23 CONTINUE
Y(223)=0.
DO 24 I5=4, I4, 2
J4=I5+500
J5=I5+501
24 Y(223)=Y(223)+(2.*C(J4))+4.*C(J5)
IF(SENSE SWITCH 1)55, 56
55 PUNCH, Y(223)
56 J6=I4+2
Y(224)=(Y(221)/3.)*(C(502)+(4.*C(503))+Y(223)+C(J6))
Y(233)=Y(224)+Y(232)
PUNCH, Y(233), Y(204), Y(205), Y(224)
PUNCH, Y(207), Y(208), Y(209), Y(210)
IF(SENSE SWITCH 1)57, 58
57 PUNCH, Y(229), Y(230), Y(231), C(409)
PUNCH, Y(217), Y(221), Y(502), C(502)
58 PUNCH, Y(211), Y(212), Y(213), Y(206)
J7=0
PUNCH, J7
GO TO 1

```